

## Low-spin states in $^{200}\text{Hg}$ studied with the $(n, \gamma)$ reaction\*

D. Breitig,<sup>†</sup> R. F. Casten, and G. W. Cole

Brookhaven National Laboratory, Upton, New York 11973

(Received 14 August 1973)

The level scheme of  $^{200}\text{Hg}$  has been studied by thermal and resonance neutron capture. The low-energy region has been measured with the high-resolution bent-crystal spectrometer at Risø, Denmark. The medium- and high-energy  $\gamma$  rays, coincidence spectra, and  $\gamma$ - $\gamma$  angular correlations were measured at the Brookhaven National Laboratory (BNL) high flux beam reactor. Primary transitions from resonance capture in  $^{199}\text{Hg}$  were studied with the fast chopper facility at BNL. Out of  $\sim 520$  observed transitions,  $\sim 330$  were placed in a level scheme containing 60 levels below 3.3 MeV. Many of these states are new and a great number of new  $I^\pi$  assignments was made. In particular  $I^\pi = 0^+$  was assigned to a level at 1515 keV. Four  $1^-$  states between 2.4 and 3 MeV are suggested. Possible explanations of their low excitation energy are offered. The simplest require and therefore suggest oblate shapes in  $^{200}\text{Hg}$ , at least for excitations involving the unique parity orbitals. A very systematic behavior of the level feeding by nonprimary transitions was found in this nucleus and was compared to simple statistical predictions. A detailed comparison was made with model calculations for core-coupled proton states. The most likely candidates for these states are:  $2_1^+$  368 keV,  $2_2^+$  1254 keV,  $2_3^+$  1575 keV,  $0_2^+$  1515 keV,  $1_1^+$  1570 keV,  $3_1^+$  1659 keV. The possibility of a reduced central density of  $^{200}\text{Hg}$  is discussed.

[ NUCLEAR REACTIONS  $^{199}\text{Hg}(n, \gamma)$ ,  $E = \text{thermal, 33.5, 129.7, and 175.1 eV}$   
measured  $I_\gamma$ ,  $\gamma$ - $\gamma$  coin( $\theta$ ) in  $^{200}\text{Hg}$ .  $^{200}\text{Hg}$  deduced levels, transitions,  $J, \pi$ ,  
ICC, multipolarities,  $\delta$ . ]

### I. INTRODUCTION

The structure of the nucleus  $^{200}\text{Hg}$  has been studied very extensively in the past years using various kinds of reactions. The first insight into the decay of the lower-lying levels of this nucleus came from  $\beta$ -decay studies of the neighboring isobars  $^{200}\text{Tl}$  and  $^{200}\text{Au}$ .<sup>1-5</sup> These experiments were repeated with refined techniques by several groups in the following years<sup>6-11</sup> and further information was gained from thermal neutron capture in  $^{199}\text{Hg}$ .<sup>12-18</sup> The results of the previous measurements on  $^{200}\text{Hg}$  have been compiled in Ref. 19.

In spite of this large amount of information the nucleus is still far from being understood. The fact that it lies rather close to the doubly magic  $^{208}\text{Pb}$  does not necessarily imply a simple structure as a rapid breakdown of the simple shell model is observed even in going three neutrons away from  $N=126$ .<sup>20</sup> This is also indicated by  $(d, p)$  and  $(d, t)$  experiments on odd- $A$  Hg isotopes,<sup>21</sup> which reveal a very complex filling of the shell-model orbits. More refined shell-model calculations including two proton and six neutron holes in the  $^{208}\text{Pb}$  core are at present quite difficult. A reasonable approach to the level structure of  $^{200}\text{Hg}$  seems therefore to be calculations by Alaga and Ialongo<sup>22</sup> and Covello and Sartoris<sup>23</sup> in which the two proton holes are coupled to harmonic surface vibrations.

The agreement between these model predictions and the previous experimental results was fair but left some points unexplained. One of the aims of the present experiment is therefore to clarify these discrepancies and provide further insight into the validity of the model. The predicted core-coupled states are expected to have  $I \leq 4$  and should lie below 2 MeV. In order to pick the most likely candidates out of a great number of other configurations which are neglected by the simplified model, it is necessary to get as complete information as possible on the decay and spin assignments of all low-lying levels. The  $(n, \gamma)$  reaction at thermal and resonant energies selectively populates low-spin states in  $^{200}\text{Hg}$ , and is very well suited for such a detailed study. High resolution data were obtained from a bent-crystal spectrometer measurement of the low-energy  $(n, \gamma)$  spectrum and were combined with measurements with Ge(Li) detectors which covered the energy range up to the binding energy. Coincidence and  $\gamma$ - $\gamma$  angular-correlation techniques have also been applied.

We also studied very extensively the energy region above 2 MeV, where previous results on decay and spin assignments were rather incomplete. A recent interest has been attached to this region by a theoretical calculation of Wong.<sup>24</sup> He predicts  $^{200}\text{Hg}$  to be one of the few nuclei which may have a

reduced central density (bubble) in the ground state. A consequence of this shape would be a second vibrational mode due to the inner surface of the nucleus which may occur below 3 MeV.

## II. EXPERIMENTAL PROCEDURES AND RESULTS

### A. High resolution $(n, \gamma)$ measurement of the low-energy spectrum

This measurement was carried out with the Risø bent-crystal spectrometer which provides the highest available resolution for  $\gamma$  rays up to about 1 MeV. Details of the apparatus and the measuring procedure have been given elsewhere.<sup>25</sup> The target consisted of 37 mg of HgS with an isotopic enrichment of ~97% for  $^{199}\text{Hg}$ . The line width for this very thin source was only 1.1" of arc. This corresponds to a resolution full width at half maximum (FWHM) of about

$$\Delta E[\text{keV}] = 2 E^2[\text{MeV}]/n,$$

where  $n$  is the order of reflection. For strong lines, observed in the fifth order of reflection, this would give resolutions of ~400 eV at 1 MeV or 36 eV at 300 keV. The energy resolution has been improved by almost a factor of 8 over an earlier measurement of  $^{199}\text{Hg}(n, \gamma)$  with the same instrument.<sup>13</sup>

The spectra recorded in five orders of reflection, covered  $\gamma$ -ray energies from about 70 to 2100 keV. Figure 1 shows a small energy range in three orders of reflection.

The measured spectra were fitted with the help of the computer program ASYMFIT<sup>26</sup> using a smooth background function (typically a straight line) and a Gaussian curve as the best approximation for the line shape. The fitting procedure, the corrections for nonlinearity in the angular scale, and the final averaging process are described in detail in Ref. 26. A total of 376 lines was found, of which the weakest detectable corresponds to 0.2  $\gamma$  rays per  $10^4$  neutron captures, assuming that the strong 368-keV line has about 80% of the total intensity per  $n$  capture.<sup>19</sup> This latter line had in the second reflection order a peak counting rate of  $1.6 \times 10^4/\text{s}$  and a sensitivity [peak/(background)<sup>1/2</sup>] of about  $5 \times 10^4$ . The energy calibration was performed using the precise x-ray energy values of Bergvall<sup>27</sup> for the  $K_{\alpha 1}$  and  $K_{\alpha 2}$  lines of  $^{200}\text{Hg}$ . The intensities were corrected for the reflectivity of the crystal, absorption between source and detector, self-absorption in the  $\gamma$ -ray source, and detector efficiency.

### B. Measurement of the medium-energy region with a Ge(Li) detector

Above about 1 MeV the resolution of a good Ge(Li) detector becomes comparable to the resolution of the bent-crystal spectrometer. In addition, with increasing energy the Ge(Li) diode efficiency decreases more slowly than that of the crystal spectrometer. Therefore the energy region of 1–3 MeV was investigated with a coaxial Ge(Li) detector of 40-cm<sup>3</sup> volume, which had a resolution of about 2.5 keV for the  $^{60}\text{Co}$  lines. The detector was installed at 90° to an external beam of the BNL high flux beam reactor. The target consisting of 70 mg HgO enriched to 97% in  $^{199}\text{Hg}$  received a thermal neutron beam current of about  $5 \times 10^5$  n/s. Due to the thickness of the target and the high thermal cross section (~2000 b) of  $^{199}\text{Hg}$ , all neutrons were captured. A portion of the spectrum taken in ~66 h is shown in Fig. 2. The energy calibration was made by comparison with bent-crystal spectrometer energies for some of the strongest lines between 1 and 2 MeV. Above 2-MeV strong lines were used whose placement in the level scheme was certain: Their energies were deduced from level energy differences which were accurate to better than 0.1 keV on the basis of low-energy transitions. Peak intensities were corrected for detector efficiency and absorption and normalized to the relative intensities of the bent-crystal spectrometer measurement. The results of the Ge(Li) and the bent-crystal spectrometer measurements are combined in Table I. Altogether, ~500 lines were found in the energy region from 70–3000 keV. Below 1 MeV only the bent-crystal spectrometer data were taken, above

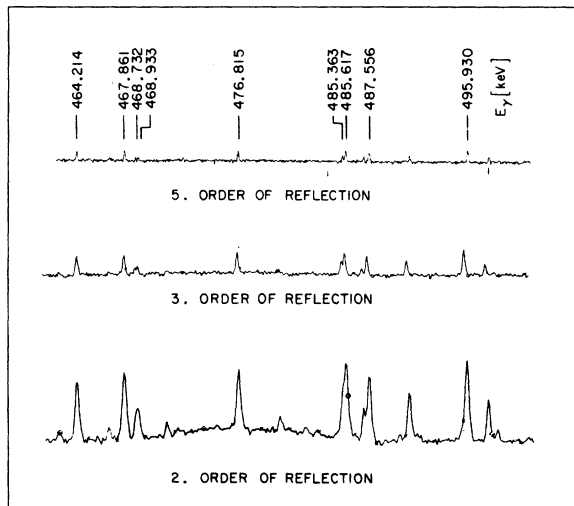


FIG. 1. Part of the low-energy  $(n, \gamma)$  spectrum of  $^{200}\text{Hg}$  measured with the Risø bent-crystal spectrometer.

2 MeV the table shows the Ge(Li) results. From 1–2 MeV the listed transition energies are adopted values from both measurements. The energy errors given in brackets are on the last digits. Intensity errors are in percent and are not shown if >40%. Lines placed in the level scheme are marked with x, those placed more than once are marked with \*.

### C. Coincidence measurements

A second Ge(Li) detector of 30-cm<sup>3</sup> volume placed at 180° to the 40-cm<sup>3</sup> detector was gated

on the very intense 368-keV line to measure the spectrum below 3 MeV coincident with this transition which leads from the first excited 2<sup>+</sup> state to the ground state. Almost all levels found have a strong branch leading eventually to the 368-keV level. Therefore, lines which are strong in the singles and not seen in this coincidence spectrum can be considered with high certainty as ground-state transitions. To eliminate lines which are coincident with the background under the 368-keV line (Compton spectra of higher-energy lines), a run was made setting the gating window with equal width near 368 keV.

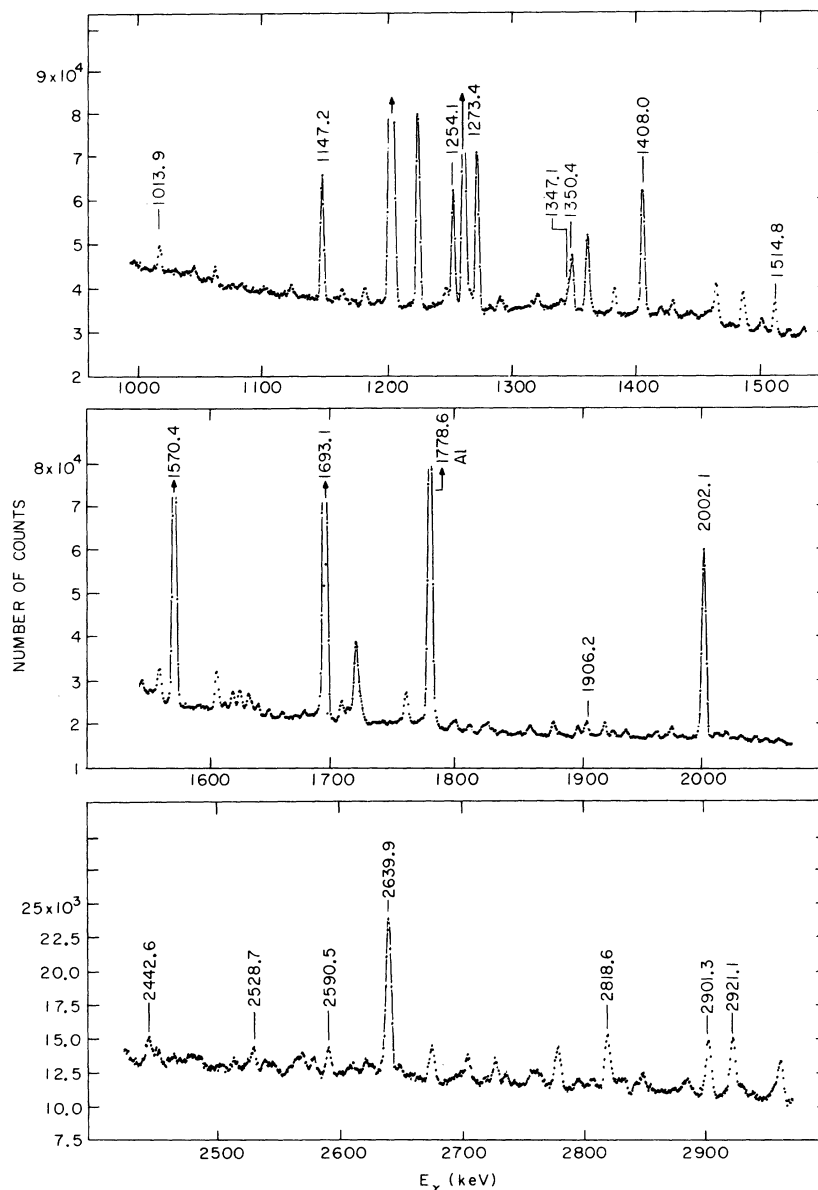


FIG. 2. Parts of the ( $n, \gamma$ ) spectrum of <sup>200</sup>Hg measured with a Ge(Li) detector.

TABLE I. Low-energy  $\gamma$  rays following thermal-neutron capture in  $^{199}\text{Hg}$ . Comments on lines: "q," questionable line; "u," unresolved multiplet; "i," possibly impurity line; "m," energy is taken from Mampe *et al.* (Ref. 18); "r," line was only seen in low-energy resonance capture spectra. Lines marked "x" are placed in the level scheme, those marked with "\*" are placed more than once.

Comment	Energy <sup>a</sup> (keV)	Intensity <sup>b</sup> (rel)	$\alpha_{\text{exp}}^c$	Multipolarity <sup>d</sup>	Comment	Energy <sup>a</sup> (keV)	Intensity <sup>b</sup> (rel)	$\alpha_{\text{exp}}^c$	Multipolarity <sup>d</sup>
q	76.857(4)x	2.1(30)				204.477(8)x	0.23(10)		
q	83.639(9)	3.9				206.083(9)	0.09(15)		
q	97.548(9)	2.5				214.44(2)	0.04		
q	97.761(10)	2.3				215.598(9)	0.13(15)		
q	99.779(10)	2.1				215.743(13)x	0.06(25)		
q	113.24(2)	1.0				223.494(7)	0.11(15)		
q	115.714(9)x	1.4(30)				224.750(6)x	0.19(10)		
q	130.26(2)	0.4				225.885(6)x	0.65(6)	63(20)	M1
	137.50(2)x	0.4				227.65(2)	0.04(35)		
	138.471(16)x	0.4				235.516(10)	0.05(20)		
	140.898(12)x	0.5(30)				241.356(12)x	0.05(35)		
	144.639(10)*	1.1(15)				241.425(10)x	0.07(25)		
	148.026(4)x	0.95(10)				243.411(7)x	0.25(8)		
	148.500(6)*	0.17(20)				245.223(8)	0.16(15)		
i	151.932(5)x	0.28(15)				247.35(2)	0.03(30)		
	156.634(12)	0.05				249.265(14)	0.03(35)		
	159.299(6)	0.32(20)				250.778(13)	0.04(25)		
q	160.49(3)	0.11				251.969(7)x	0.72(6)		
q	160.659(11)*	0.07				252.356(7)x	0.41(7)		
	162.434(13)	0.05				253.991(15)x	0.04(30)		
q	164.544(6)x	0.39(10)				255.75(3)	0.05(25)		
q	164.658(15)	0.04			q	268.18(3)	0.03		
i	167.483(7)	0.11(20)			q	268.49(3)x	0.03		
q	182.53(3)x	0.07				270.530(12)x	0.07(20)		
q	182.70(3)	0.06				271.68(2)x	0.06(15)		
q	185.911(10)	0.06(30)				272.109(8)*	0.33(7)	60	M1
q	185.98(2)	0.04				275.497(12)x	0.06(15)		
q	186.771(13)x	0.05(35)				278.17(3)	0.07(25)		
q	189.96(2)	0.03				278.274(13)	0.09(25)		
q	190.24(2)	0.03				278.88(3)	0.03(35)		
	197.45(2)	0.03				281.08(2)*	0.05(20)		
	201.91(2)x	0.04(35)				283.88(3)x	0.04(30)		
	202.966(13)	0.06(30)				286.518(13)x	0.07(15)		
	203.135(7)x	0.56(10)	76(22)	M1		287.182(10)	0.11(10)		
	203.832(12)x	0.06(30)				287.620(13)	0.06(20)		

TABLE I (Continued)

Comment	Energy <sup>a</sup> (keV)	Intensity <sup>b</sup> (rel)	$\alpha_{\text{exp}}^c$	Multipolarity <sup>d</sup>	Comment	Energy <sup>a</sup> (keV)	Intensity <sup>b</sup> (rel)	$\alpha_{\text{exp}}^c$	Multipolarity <sup>d</sup>
	289.425(9)x	1.30(6)	37(10)	M1		352.353(12)x	0.27(11)		
	298.34(4)	0.03(35)				353.07(5)	0.04(35)		
q	298.75(6)	0.04				356.44(4)	0.09(25)		
q	299.53(6)	0.05				359.48(4)x	0.07(25)		
	299.887(12)x	0.09(15)				363.72(8)x	0.04(40)		
	301.963(13)*	0.07(15)				367.942(10)x	1180(4)	3.6(7)	E2
	306.618(11)x	0.18(10)				376.68(2)x	0.20(25)		
	306.863(11)x	0.12(12)				376.79(2)x	0.23(20)		
	308.47(4)	0.03(40)				380.03(2)x	0.10(13)		
	308.801(11)x	0.14(10)				383.437(11)x	0.32(8)		
	309.209(8)x	0.55(6)	>47	M1		387.345(9)x	1.59(6)	22(5)	M1
	312.613(13)x	0.08(12)				392.524(17)x	0.12(11)		
	313.23(3)x	0.04(25)				395.97(4)x	0.06(25)		
	316.176(8)x	1.12(6)	33(15)	M1		397.01(2)x	0.16(13)		
	317.74(10)	0.03				397.765(14)x	0.29(11)		
	318.03(8)	0.04				398.249(9)x	3.70(5)	21(4)	M1
	319.566(15)x	0.08(15)				398.63(2)x	0.22(14)		
	321.55(3)x	0.06(20)				399.65(5)	0.04(40)		
	322.57(5)	0.05(25)				404.94(4)x	0.06(17)		
	325.31(4)	0.04(30)				408.556(10)x	1.34(6)	18(5)	M1
	329.27(4)	0.03(35)				409.63(3)x	0.09(18)		
	330.303(16)x	0.11(15)			q	414.41(7)x	0.04		
	330.84(3)x	0.06				415.50(3)	0.09(13)		
	331.34(3)x	0.05(25)				419.828(10)x	1.81(6)	12(3)	M1
	332.67(4)x	0.05(30)				423.24(3)x	0.17(14)		
	337.51(2)x	0.05(20)				427.79(3)	0.14(13)		
	338.75(2)x	0.21(8)				428.45(3)x	0.13(13)		
	340.03(2)x	0.09(12)				429.79(7)	0.06		
	341.375(12)x	0.21(8)				430.368(10)x	4.72(6)	13(3)	M1
	342.185(14)	0.21(8)				437.03(5)	0.05		
	342.42(3)	0.05(35)			q	437.56(13)	0.06(40)		
	342.939(12)x	0.39(10)				439.52(4)*	0.08(25)		
	343.38(2)x	0.07(15)				445.686(14)	0.51(8)		
	346.406(14)x	0.19(10)				448.91(2)x	1.09(8)		
	351.27(2)*	0.31(12)			q	452.30(14)	0.07		

TABLE I (Continued)

Comment	Energy <sup>a</sup> (keV)	Intensity <sup>b</sup> (rel)	$\alpha_{\text{exp}}^c$	Multipolarity <sup>d</sup>	Comment	Energy <sup>a</sup> (keV)	Intensity <sup>b</sup> (rel)	$\alpha_{\text{exp}}^c$	Multipolarity <sup>d</sup>
	453.60(16)x	0.07				521.41(7)x	0.13(30)		
	455.13(4)x	0.11(15)				532.53(6)	0.11(25)		
	456.10(5)	0.07(25)				533.48(3)	0.47(9)	>13	M1
	458.80(9)	0.07(35)				534.48(3)x	0.17(18)		
	460.76(5)x	0.09(25)				535.01(5)	0.14(20)		
	461.16(9)	0.07(30)				537.30(5)	0.20(16)		
	462.94(5)	0.08(25)				540.948(16)x	9.79(6)	6.4(1.0)	M1
	464.214(12)x	1.31(6)	5	E2 + M1		544.21(7)x	0.10(20)		
	466.72(3)x	0.10(25)				546.10(2)x	0.71(7)	9.4(3.5)	M1
	467.86(2)*	1.65(6)	14(4)	M1	q	546.99(12)	0.07		
	468.73(3)	0.29(25)				551.93(8)	0.17(30)		
	468.93(2)x	0.35(20)			q	552.49(19)	0.08		
	471.19(3)x	0.14(15)				553.18(2)x	1.25(7)	5.6(2.0)	M1
	472.12(6)x	0.07(30)				556.58(2)x	3.38(6)	5.0(1.3)	M1(+15%E2)
	475.08(4)*	0.10(20)				558.61(5)x	0.15(20)		
	476.815(13)x	1.95(6)	2	E2		562.57(3)	0.53(8)		
	480.24(3)x	0.22(11)				563.63(9)x	0.11(30)		
	482.32(6)	0.08(30)				564.19(5)x	0.17(20)		
	483.34(9)x	0.07				566.15(5)x	0.26(14)		
	485.36(2)x	0.98(11)	>1.7			568.04(7)x	0.13(25)		
	485.62(2)x	2.42(8)	>5.6	E2 + M1, M1	q	571.8(3)	0.09		
	486.44(7)x	0.08(35)				573.41(4)x	0.27(13)		
	487.12(3)x	0.52(11)				577.98(6)x	0.20(35)		
	487.56(2)x	1.81(7)	>4.8	E2 + M1, M1		579.300(17)x	27.8(6)	1.44	E2
	490.95(2)x	1.16(6)	4.4	E2 + M1		583.00(10)	0.08(35)		
	491.70(6)	0.10(25)			u	585.18(8)	0.10(40)		
	495.48(8)	0.09(40)				586.98(12)x	0.09(35)		
	495.93(2)x	3.05(6)	6.1	M1(+E2)		587.88(4)x	0.27(12)		
	497.81(2)*	0.86(7)				588.96(6)x	0.17(17)		
	498.63(4)x	0.18(13)				591.66(3)x	1.22(7)	2.7	E2 + M1
	502.83(4)	0.22(11)				596.06(3)x	0.43(10)		
	505.23(3)x	0.14(17)				597.41(4)x	0.31(14)		
	516.35(3)x	0.27(15)				598.35(3)x	0.66(9)	>2.5	E2 + M1, M1
	517.14(7)x	0.15(25)			q	598.99(13)	0.14		
	520.91(5)x	0.21(17)				599.93(11)	0.09(35)		

TABLE I (Continued)

Comment	Energy <sup>a</sup> (keV)	Intensity <sup>b</sup> (rel)	$\alpha_{\text{exp}}^c$	Multipolarity <sup>d</sup>	Comment	Energy <sup>a</sup> (keV)	Intensity <sup>b</sup> (rel)	$\alpha_{\text{exp}}^c$	Multipolarity <sup>d</sup>
	600.82(4)x	0.37(11)			q	687.1(3)	0.20		
	601.48(5)x	0.27(16)				688.94(3)x	9.2(7)	3.3(7)	M1
	602.73(7)x	0.18(20)				690.28(6)x	0.60(25)		
	607.26(10)	0.08(30)				694.14(5)x	0.51(17)		
	608.22(9)x	0.19(35)				695.72(20)x	0.17		
	608.93(13)	0.21				700.17(15)x	0.27(35)		
	609.94(13)	0.11(40)				701.56(3)x	8.2(8)	0.3 < $\alpha$ < 1.0	E1, E2
	612.12(3)x	2.48(8)	<1.6			703.82(5)*	1.22(14)		
	613.55(5)x	0.25(20)				706.26(15)	0.20(30)		
	615.54(4)x	0.82(20)				709.32(12)	0.23(25)		
	615.82(10)x	0.49				710.22(11)	0.30(25)		
	623.24(3)	0.76(7)				710.93(12)x	0.21(40)		
	626.52(10)x	0.13(30)				711.70(5)x	0.85(9)		
	628.80(3)x	1.88(7)	3.7(1.0)	M1 + (15%E2)		713.94(10)x	0.26(18)		
	631.50(9)x	0.14(25)				718.04(10)x	0.50(25)		
	632.85(5)x	0.19(20)				718.55(13)x	0.36(30)		
	634.66(10)*	0.17(25)			q	720.21(5)x	0.78(9)		
	635.86(16)*	0.14				721.0(8)x	0.2		
	636.76(16)	0.09				722.2(5)x	0.2		
	638.53(11)	0.14				724.78(10)x	0.21(25)		
	639.11(4)x	0.80(8)				728.45(7)x	0.81(10)		
	643.29(4)x	0.62(10)				733.4(3)x	0.43(25)		
	644.93(5)	0.23(16)				738.5(2)x	0.25		
	646.17(7)x	0.19(18)				739.05(16)x	0.41(30)		
u	649.24(8)	0.21(17)				743.52(8)	0.53(13)		
	651.4(3)x	0.19(30)				745.22(12)	0.26(25)		
u	652.91(8)x	0.21(17)				747.30(9)x	0.38(18)		
	655.59(5)x	0.32(15)				748.84(10)x	0.48(19)		
	659.01(3)x	1.44(10)				749.9(2)x	0.18(35)		
	661.36(3)x	80.5(7)	1.02(14)	E2		755.92(18)	0.18(40)		
	674.29(7)x	0.27(30)				757.01(6)*	1.23(10)		
	676.15(3)x	2.57(8)	2.9(9)	M1 + 25%E2		759.30(11)x	0.34(17)		
	677.45(7)x	0.56(14)				761.43(12)*	0.59(35)		
	681.87(8)x	0.37(25)				762.10(19)	0.33		
	685.19(12)x	0.20(30)				778.89(14)	0.29(25)		

TABLE I (Continued)

Comment	Energy <sup>a</sup> (keV)	Intensity <sup>b</sup> (rel)	$\alpha_{\text{exp}}^c$	Multipolarity <sup>d</sup>	Comment	Energy <sup>a</sup> (keV)	Intensity <sup>b</sup> (rel)	$\alpha_{\text{exp}}^c$	Multipolarity <sup>d</sup>
q	780.02(18)	0.44				980.2(5)x	0.9		
	780.96(11)*	0.28(25)				992.35(17)x	1.35(14)		
	783.71(4)x	3.00(8)	<1.4		u	996.5(7)x	0.6(40)		
	784.9(3)x	0.24				1002.5(3)	1.2(35)		
	787.10(4)x	3.10(9)	>1.9	M1		1008.7(4)x	1.0		
	788.77(6)x	1.13(14)				1010.2(5)	0.8		
	789.73(19)	0.37(35)			q	1013.9(8)	4.1(15)	0.43(13)	E2
	796.41(6)x	1.67(8)	2.9(8)	M1		1022.5(4)x	0.7		
	797.4(2)x	0.32(35)				1027.1(3)x	1.3(30)		E2 (+M1)
	799.90(18)x	0.57(30)				1034.9(10)x	0.8		
	807.20(5)x	2.86(7)	1.8(5)	M1 + 25%E2		1038(1)	0.8		
	818.33(11)*	0.63(17)				1042.4(3)x	1.8(25)	1.2	M1
	823.95(14)x	0.43(30)				1054.7(4)x	1.0(40)	1.9	M1
	828.27(4)x	4.9(7)	2.0(5)	M1	u	1059.6(2)*	2.0(25)	<0.9	
u	837.7(3)	0.3				1070.0(4)x	0.4		
	851.36(4)x	9.1(7)	1.6(3)	M1 + 25%E2		1074.1(4)	0.4		
u	854.2(2)x	0.60(35)				1081.3(3)*	0.7(30)		
	860.6(2)x	0.49(35)				1100.3(5)	0.7		
	861.71(12)x	0.95(19)			q	1116(1)x	0.4		
u	872.93(14)*	0.69(18)				1121.4(2)	2.5(25)	1.2(4)	M1
	886.20(4)x	50.7(7)	0.81(11)	E2 + 20%M1		1137.6(6)	0.7		
	890.0(5)x	0.4				1147.20(8)x	23(10)	0.41(6)	E2
q	896.7(2)x	0.2				1158.3(7)x	1.1(30)		
	898.56(7)x	2.6(9)	0.80(32)	E2 (+20%M1)		1163.5(3)x	2.8(20)	0.78	M1 (+E2)
	901.69(17)	0.6				1167.0(7)x	0.8		
	903.5(2)x	0.4				1172.8(5)	1.0(40)		
	904.36(12)	1.4(30)				1180.4(4)x	1.0(40)		
	905.3(4)*	0.6			m	1181.9x		>5.1	E0
	911.5(6)x	0.85(35)				1192.9(6)x	0.8		
	917.9(3)x	0.80(25)				1202.35(7)x	37(10)	0.71(13)	M1 + 20%E2
	935.45(8)x	2.15(12)	0.94	E2 + M1		1205.75(7)x	41(9)	0.88(17)	M1
	945.4(3)	0.59(30)				1225.44(8)x	40(8)	0.78(10)	M1
	947.34(17)	0.6			r	1237x			
	957.19(13)*	0.86(18)				1247.3(3)*	3.4(20)		
	975.15(7)x	5.4(9)	1.00(23)	M1 + 40%E2		1254.14(10)x	23(9)	0.33(7)	E2



TABLE I (Continued)

Comment	Energy <sup>a</sup> (keV)	Intensity <sup>b</sup> (rel)	$\alpha_{\text{exp}}^c$	Multipolarity <sup>d</sup>	Comment	Energy <sup>a</sup> (keV)	Intensity <sup>b</sup> (rel)	$\alpha_{\text{exp}}^c$	Multipolarity <sup>d</sup>
	1262.96(8)x	65(8)	0.62(7)	M1 + 20%E2		1557.7(3)x	10(20)	0.37	M1
	1266.9(6)x	2.4				1570.45(15)x	93(10)	0.36(4)	M1
	1273.43(10)x	33(9)	0.58(8)	M1 + 30%E2		1589.8(5)	0.8		
	1283.9(7)x	1.1				1604.5(2)x	12(15)	0.32(8)	M1 + 40%E2
	1291.1(6)x	3.3(30)				1610.9(6)*	2.4(30)		
	1294.6(6)x	1.7			u	1623.5(3)x	6.7(20)	<0.3	
	1318.0(6)x	1.9(30)				1630.7(4)x	5.6(20)	>0.18	E2, M1
	1322.4(3)x	3.5(25)	0.7	M1		1633.6(7)	2.9(40)		
u	1337.4(1.5)x	1.8			u	1638.3(5)x	3.5(25)		
	1341.7(5)x	2.9(25)	<0.7			1647.2(3)x	1.9(30)		
	1347.1(5)x	5.8(40)				1658.2(3)x	1.4(30)		
	1350.4(2)x	12.5(10)	0.54(10)	M1 + (15%E2)	m	1667.8x	<1	>2.5	E0
	1363.2(2)x	18(12)	0.64(13)	M1	u	1669.6(1.5)	~1		
	1366.8(7)*	1.8				1676.3(3)x	3.0(25)		
	1385.0(3)*	6.0(20)	0.40(10)	E2 + 45%M1	u	1681.1(1.5)	1.9		
	1408.0(2)x	32(10)	0.40(6)	E2 + 45%M1		1685.5(1.0)	2.8(40)		
m	1420.5	<1	>2	E0		1693.13(14)x	165(10)	0.31(4)	M1 (+E2)
	1422.4(3)*	1.5(30)				1699.1(1.0)x	~1		
	1426.4(6)	1.1				1706.6(3)x	7.6(15)	<0.17	
u	1432.2(2)*	4.0(20)	0.40			1711.7(5)	4.8(25)		
	1442.5(1.0)x	~1			q	1715.2(1.0)x	~1		
	1447.5(7)x	1.9(30)				1718.6(4)x	23(15)	>0.27	M1
u	1458.2(1.5)	1.2				1722.2(6)	8.2(25)		
	1462.5(1.5)x	1.9(30)			q	1733.7(1.0)x	~1		
	1467.6(3)x	9.4(15)	0.36(10)	M1 + E2	q	1740.2(1.5)	~1		
	1479.6(1.5)x	~1			q	1745.9(1.5)x	~1		
q	1488.5(4)x	10(20)	0.28(10)	E2		1754.6(7)*	2.6(40)		
	1503.2(4)x	6.5(20)	0.18	E2	u	1759.3(3)*	11(10)	<0.11	
	1514.8(3)x	9(20)	0.70(17)	? + E0		1771.9(7)	2.9(40)		
	1525.9(3)	1.8(30)				1783.3(1.0)	~1.5		
	1538.2(5)*	2.0(30)				1796.0(7)	2.1		
	1543.1(5)	6(20)				1799.2(5)x	3.3(30)		
	1546.1(7)	2.5				1811.2(4)	3.0(20)		
	1550.1(6)	3.0(30)				1822.3(7)x	2.1(35)		
	1553.7(7)	2.5				1825.9(5)	3.3(25)		

TABLE I (Continued)

Comment	Energy <sup>a</sup> (keV)	Intensity <sup>b</sup> (rel)	$\alpha_{\text{exp}}^c$	Multipolarity <sup>d</sup>	Comment	Energy <sup>a</sup> (keV)	Intensity <sup>b</sup> (rel)	$\alpha_{\text{exp}}^c$	Multipolarity <sup>d</sup>
u	1829.8(7)	1.8(35)				2289.6(7)	~1.5		
u	1838.1(1.5)	1.5				2296.3(3)x	9.5(10)	0.15(5)	M1
m	1857.4x	<1.5	>7	E0		2304.7(7)	1.1(35)		
u	1860.4(3)	4.7			u	2323.5(4)x	3.5(25)	0.06	
u	1879.3(3)x	~1.2				2346.5(6)	2.3(25)		
	1906.2(3)x	5.6(15)	0.11	E2		2365.2(7)	1.6(30)		
	1921.1(3)x	4.4(15)	<0.14			2370.0(3)x	3.3(20)	0.12	M1 (E2)
	1928.2(3)x	1.9(30)				2401.9(4)	2.4(20)	0.09(4)	E2
	1957.6(7)	1.3			u	2423.7(7)	3.2(30)	<0.06	
	1963.5(4)x	2.6(20)			u	2442.6(3)x	6.2(15)	0.02	E1
	1970.9(7)	1.3				2449.8(5)	1.6		
	1975.8(3)x	3.9(20)	0.38(16)	M1	u	2462.6(1.5)x	1.9(40)	0.12	
u	1984.5(7)	1.6(35)				2468.0(1.5)	1.6		
	2002.1(2)x	77(10)	0.18(3)	M1+E2		2475.8(1.5)	2(35)		
	2020.6(7)x	3.4(20)	0.18	M1+E2		2480.2(1.5)	2(35)		
	2032.6(4)	2.0(30)				2485.3(1.5)x	2(35)	0.11	E2+M1
	2044.2(5)*	2.0(30)			u	2502.6(1.5)	1.7		
	2063.7(6)	1.4				2513.1(7)	2(30)		
	2082.9(7)	1.7				2524.3(7)	2(35)		
	2093.6(4)x	4.2(20)	<0.15			2528.7(4)	4.6(15)	0.05(2)	E1
	2107.8(3)	4.5(20)	<0.15			2538.0(5)	2.5(25)		
m	2118.4	<1.5	>0.8	E0	u	2544.5(7)	2.5(30)		
	2123.9(7)x	4.2(20)	0.12	E2, M1		2559.0(1.0)	1.3		
u	2139.7(3)	5.0(20)	<0.13			2564.8(7)	2.9(25)	0.04	E1
	2161.4(7)	3.5(35)				2569.1(5)x	4.2(20)	<0.03	E1
	2180.8(5)	5.0(20)	0.13	E2		2578.4(3)	3.4(20)	<0.04	E1
	2188.7(6)x	4.3(20)	0.32(10)	M1		2590.5(3)x	6.1(10)	<0.02	E1
	2194.4(5)	2.2				2606.7(1.0)	1.7(35)		
	2204.6(1.0)	1.5(35)				2611.0(7)x	3.0(20)		
	2240.6(7)x	3.0(30)				2620.9(4)	3.5(25)		
q	2246(2)x					2625.5(7)	2.6(30)		
	2251.4(1.0)	4.8(35)				2639.9(2)x	33(10)	0.105(15)	M1
	2259.5(5)	5.6(20)	0.13(3)	E2+M1		2648.9(5)	3.0(20)		
	2271.5(4)x	19(15)	0.11(2)	E2		2695.0(1.5)	1.5		
	2283.0(4)	6.1(20)	<0.06	E1 (E2)		2699.3(1.5)	1.5		

TABLE I (Continued)

Comment	Energy <sup>a</sup> (keV)	Intensity <sup>b</sup> (rel)	$\alpha_{\text{exp}}^c$	Multipolarity <sup>d</sup>	Comment	Energy <sup>a</sup> (keV)	Intensity <sup>b</sup> (rel)	$\alpha_{\text{exp}}^c$	Multipolarity <sup>d</sup>
	2704.6(3)	1.8				2921.1(3)x	16(10)	0.064(12)	E2
	2727.2(3)	4(25)				2928.6(1.0)	2.9(30)		
	2735.8(5)	2.7(20)				2937.2(1.0)x	1.5		
q	2742.7(7)	1.4				2953.8(1.0)	2.0(30)		E1
	2756.2(1.5)	3.2				2960.2(3)x	9.5(15)	<0.013	
	2764.0(1.5)x	1.8				2978.5(6)x	3.0(20)		M1
u	2794.5(4)x	2.4(30)				2985.8(3)	3.5(20)	0.08(3)	
	2806.5(4)	2.4(30)				2993.8(5)	2.0(25)		E1
	2818.6(3)x	12(10)	0.063(15)	E2		3033.6(4)	10.4(20)	<0.016	E2
u	2827.4(1.0)	2.8(30)				3051.1(8)	6.7(20)	0.058(25)	M1
	2831.8(1.0)	2.8(30)				3074.2(6)x	5(20)	0.074(22)	
u	2847.3(6)x	4.2(20)				3093.1(1.2)	2.9(30)		
	2853.8(1.0)x	1.4				3112.2(1.0)	3.6(30)		M1
q	2862.4(1.5)x	0.5				3185.8(4)x	30(10)	0.072(10)	E2
	2872.7(1.0)	1.4				3216.9(8)	9.3(20)	0.058(20)	
	2880.7(1.0)	2.8(35)				3263.3(1.5)	2.6		M1
	2883.4(5)	3.3(30)				3269.4(6)x	6.7(20)	0.10(3)	M1
	2901.3(3)x	14(10)				3288.9(4)x	32.3(10)	0.078(12)	M1

<sup>a</sup> The energy errors given in parentheses are on the last digits.

<sup>b</sup> The intensity errors are in percent and are only shown if  $\leq 40\%$ . Some intensities were corrected for superimposed escape peaks.

<sup>c</sup> Conversion coefficients (in units of  $\alpha_{\text{exp}} \times 10^4$ ) were determined using the ( $n, ce$ ) intensities of Ref. 17 below 1 MeV and of Ref. 18 above this energy. For the 1027-keV line the results of Ref. 40 were used. The relative scales of  $\gamma$  and electron intensities were connected by assuming pure E2 character for the 579-keV line. The errors given in parentheses are on the last digits and are not given if  $> 50\%$ . In case of closely lying  $\gamma$  lines not separated in the ( $n, ce$ ) spectrum, limits are given for the stronger line.

<sup>d</sup> Multipolarities were determined using the theoretical conversion coefficients of Ref. 32. Parentheses indicate that the multipolarity is less certain or that in case of mixed transitions the part in parentheses may be zero if the errors are considered.

TABLE II.  $\gamma$ - $\gamma$  angular correlation results.

Transition energy (keV)	R		Initial level	Initial spin	Multipolarity <sup>a</sup>	Sign $\delta$ <sup>b</sup>
	W(180°)	W(135°)				
661.4	2.93 ± 0.30		1029	0 <sup>+</sup>	E2	
886.2	1.46 ± 0.22		1254	2 <sup>+</sup>	E2 + (20 ± 10)%M1	+
1147.2	2.97 ± 0.50		1515	0 <sup>+</sup>	E2	
1202.4	1.00 ± 0.10		1570	1 <sup>+</sup>	M1 + (20 <sup>+30</sup> / <sub>-20</sub> )%E2	+
1205.8	1.03 ± 0.10		1573	2 <sup>+</sup>	M1(E2 < 40%) <sup>c</sup>	-
1225.5	1.13 ± 0.17		1593	2 <sup>+</sup>	M1(E2 < 30%) <sup>c</sup>	
1263.0	0.79 ± 0.12		1630	1 <sup>+</sup>	M1 + (20 ± 15)%E2	(-)
1273.4	1.16 ± 0.18		1641	2 <sup>+</sup>	M1 + (30 ± 20)%E2	
1350.4	1.25 <sup>+0.75</sup> / <sub>-0.45</sub>		1718	1 <sup>+</sup>	M1 + (15 <sup>+30</sup> / <sub>-15</sub> )%E2	+
1363.2	1.30 ± 0.26		1730	2 <sup>+</sup>	M1	
1488.5	3.1 ± 1.0		1856	0 <sup>+</sup>	E2	
1514.8	0.64 <sup>+0.5</sup> / <sub>-0.35</sub>		1882	2 <sup>+</sup>	<75%E2 <sup>c</sup>	
1604.5	0.92 <sup>+0.7</sup> / <sub>-0.4</sub>		1972	2 <sup>+</sup>	M1 + (40 <sup>+40</sup> / <sub>-35</sub> )%E2	
1693.1	0.85 ± 0.09		2061	1 <sup>+</sup>	M1 + (15 <sup>+30</sup> / <sub>-15</sub> )%E2	
1906.2	1.25 <sup>+0.8</sup> / <sub>-0.5</sub>		2274	1, 2 <sup>+</sup>	E2	
2002.1	0.86 ± 0.14		2370	1 <sup>+</sup>	M1 + (35 ± 30)%E2	(+)

<sup>a</sup> From  $(n, ce)$  experiments.

<sup>b</sup> The phase convention used is the same as in Ref. 28. The large errors on R did not allow extraction of a unique sign  $\delta$  in some cases. Parentheses indicate some ambiguity; the given sign is, however, more likely than the other.

<sup>c</sup> Limits from present  $\gamma$ - $\gamma$  correlation measurement.

#### D. $\gamma$ - $\gamma$ angular correlation measurements

Several measurements of this kind were done previously for  $^{200}\text{Hg}$ .<sup>27-29</sup> However, with the exception of Ref. 29 they all dealt with  $\gamma$  rays following  $^{200}\text{Tl}$  decay. The present correlation study was performed with the main interest on the decay of 0<sup>+</sup> states in  $^{200}\text{Hg}$ , which are very weakly populated in the  $\beta$  decay.  $\gamma$  cascades of the kind 0-2-0 show a very pronounced anisotropy of the  $\gamma$ - $\gamma$  angular correlation at 180 and 135°. Therefore, a second gated spectrum was taken at an angle of 135° between the two detectors. The measuring time was in both cases about 37 h.

In Table II the results of this correlation study are given for the strongest lines. As can be seen, the ratio  $R = W(180^\circ)/W(135^\circ)$  is usually between 0.5 and 1.5 with the exception of three lines, for which it is about 3. Theoretically R should be between 0.1 and 1 for 1-2 and between 1 and ~1.5 for 2-2 transitions, depending on their E2/M1 mixing ratio  $\delta$ .<sup>30</sup> These ranges were calculated using estimated attenuation factors due to the finite detector size.<sup>31</sup> For the 0-2 transitions one calculates  $R \approx 3$ , which is in agreement with the ratios for the 661-, 1147-, and 1488-keV lines.

For most of the coincident transitions the spin and parity of the initial level were known from level scheme considerations and their M1, E2

mixing ratio could be determined by comparison of the present  $(n, \gamma)$  intensities with  $(n, ce)$  studies (see below). This often allows the extraction of the sign of  $\delta$  from the correlation measurement. The magnitudes of the  $\delta$ 's are not always uniquely determined but the possible values are consistent with the mixing ratios obtained from the conversion electron data. However, a comparison with previous directional correlation measurements<sup>28</sup> which can only be done for 2<sup>+</sup> initial states (as 1<sup>+</sup> and 0<sup>+</sup> states are too weakly populated from  $\beta$  decay) shows serious discrepancies for  $\delta$  of the 1225- and 1363-keV lines. Hattula, Helppi, and Kantele<sup>28</sup> give 65 and 50%, respectively, E2 admixture for these lines, whereas the  $(n, ce)$  data and our correlation measurements imply almost pure M1 character. The results for the sign of  $\delta$  are the same in both angular-correlation studies.

#### E. Multipolarities of the low-energy $\gamma$ transitions

On the basis of the more precise  $\gamma$  intensities the multipolarities and E2/M1 mixing for stronger transitions below 3 MeV were reevaluated. The electron intensities were taken from Schult *et al.*<sup>17</sup> for transitions below 1 MeV and from Mampe *et al.*<sup>18</sup> for transitions between 1 and 3 MeV. The relative conversion intensities  $I_{n, ce}$  were normalized to the relative  $\gamma$  intensities  $I_{n, \gamma}$  using the K-

conversion line of the 579-keV transition which has the known multipolarity  $E2$ . Theoretical conversion coefficients used to determine the multiplicities were taken from Sliv and Band.<sup>32</sup> The results are shown in Table I. At some points serious discrepancies with previously reported results were revealed and multiplicities could also be ascribed to a number of weaker lines not seen in earlier  $(n, \gamma)$  studies. Furthermore, the lower detection limit in the present  $(n, \gamma)$  measurements allowed the confirmation of the  $E0$  character of several electron lines. Specifically no  $\gamma$  lines of 1668 and 1857 keV could be found and the electron intensities of the 1182-, 1420-, 1515-, and 1546-keV lines are too large to be accounted for as  $M1$  conversion lines of nearby  $\gamma$  lines.

#### F. Resonance neutron capture with the time-of-flight spectrometer

Resonance capture was studied at the fast chopper facility of the BNL high flux beam reactor.<sup>33, 34</sup>

A natural mercury target  $12.7 \text{ cm} \times 12.7 \text{ cm} \times 0.42 \text{ cm}$ , containing 927.3 g of metallic mercury, was placed at the 48-m flight-path station.  $\gamma$ -ray spectra were measured using a  $10\text{-cm}^3$  intrinsic germanium planar diode detector, and a  $\gamma$ -ray energy resolution of 7 keV at 8 MeV was obtained. The three lowest  $^{199}\text{Hg}(n, \gamma)$  resonances were analyzed for this work: 33.5 eV ( $J^\pi = 1^-$ ), 129.7 eV ( $0^-$ ), and 175.1 eV ( $1^-$ ).<sup>35, 36</sup> The presence of the  $0^-$  resonance at 129.7 eV was of particular use, since strong primary transitions seen in this resonance serve to identify  $1^+$  levels in  $^{200}\text{Hg}$ . This criterion is not available in the thermal-capture measurements, since the compound state, dominated by a  $0^-$  bound level, may include spin-1 components.

The resonance capture spectra are shown in Fig. 3. The  $\gamma$ -ray energy scale was determined by using the precisely measured level energies obtained in the other phases of this experiment.

Table III gives the relative intensities of primary transitions in the three resonances.

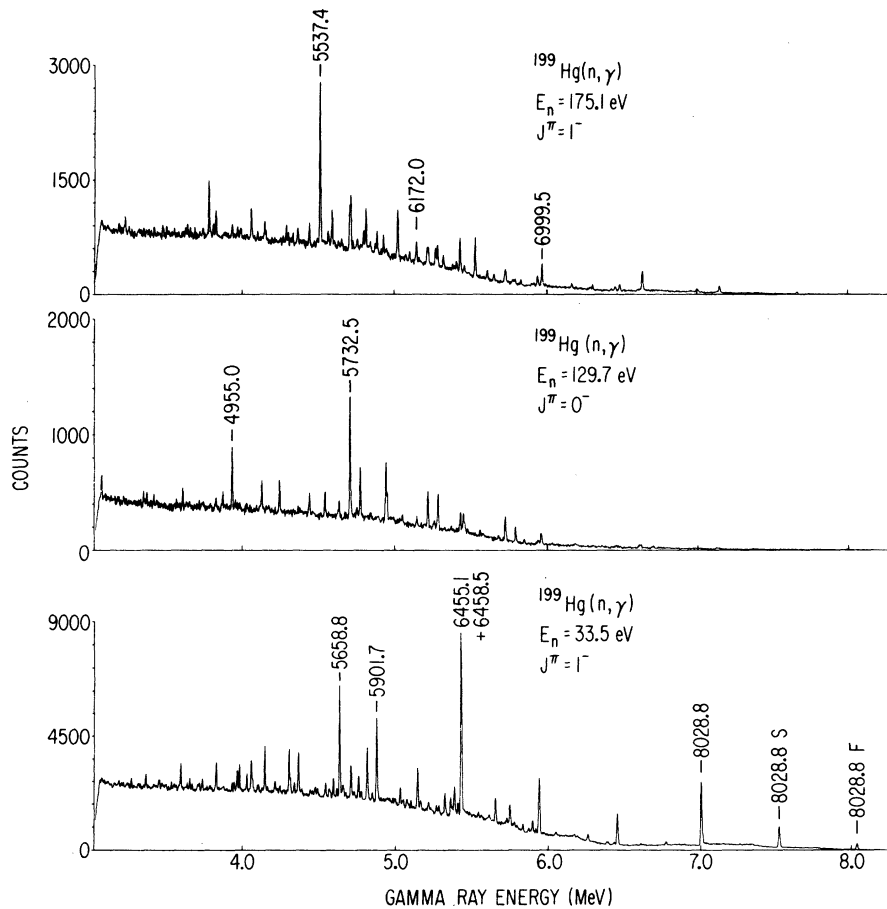


FIG. 3. High-energy  $(n, \gamma)$  spectra for three different resonances of  $^{199}\text{Hg}$ . Some full energies are given above the double escape peaks of corresponding lines.

The spectra of low-energy  $\gamma$  transitions following neutron capture in the three resonances were also measured but not analyzed in detail.

### III. LEVEL SCHEME

All available data from previous experiments were combined with the present results to construct the level scheme shown in Figs. 4-7. It

TABLE III. Relative intensities of primary transitions in resonance capture.

$E_\gamma$ (keV)	$E_{ex}$ (keV) <sup>a</sup>	33.5 eV		129.7 eV		175.1 eV	
		$I_\gamma$ <sup>b</sup>	$\frac{\Delta I_\gamma}{I_\gamma}\%$	$I_\gamma$ <sup>b</sup>	$\frac{\Delta I_\gamma}{I_\gamma}\%$	$I_\gamma$ <sup>b</sup>	$\frac{\Delta I_\gamma}{I_\gamma}\%$
8028.3	0	42.9	5	<0.30		2.3	20
7661.2	367.6	<0.2		<0.4		15.9	10
6999.5	1029.3	0.28	40	<0.4		13.3	10
6774.7	1254.1	9.5	10	0.58	70	<0.5	
6515.0	1513.8	0.66	50	<0.6		<0.5	
6458.6	1570.2 <sup>c</sup>	100	5	13.9	10	19.0	10
6436.2	1592.6	6.6	10	0.85	70	4.7	15
6398.6	1630.2	4.1	10	3.6	20	<0.7	
6387.9	1640.9	8.0	10	<0.8		<0.7	
6311.3	1717.5	2.7	30	12.5	10	8.5	15
6298.7	1730.1	<0.8		<1.0		7.5	15
6171.7	1857.1	5.1	10	<1.0		8.8	10
6055.7	1973.1	6.7	10	<1.0		1.7	40
5967.8	2061.0	4.3	10	38.8	5	7.4	15
5953.8	2075.0	1.2	40	1.3	70	7.4	15
5912.2	2116.6	2.6	15	<1.0		10.0	10
5901.6	2127.2	32.9	5	<1.0		1.7	20
5839.6	2189.2	16.0	5	2.6	40	16.7	10
5799.3	2229.5	2.7	15	26.1	5	<0.7	
5782.4	2246.4	8.9	10	1.2	70	5.1	15
5753.8	2275.0	1.7	20	<1.0		2.7	20
5739.5	2289.3	<0.3		<1.0		23.9	5
5732.1	2296.7	13.4	15	69.1	5	20.1	5
5658.5	2370.3	41.3	5	8.7	10	2.9	30
5616.4	2412.4	7.2	10	<1.0		17.7	5
5566.1	2462.7	5.3	10	16.1	5	<0.9	
5536.3	2492.5	<0.5		2.4	30	71.7	5
5465.8	2563.0	1.6	30	<1.0		8.9	10
5388.4	2640.4	17.6	5	3.3	30	11.1	10
5336.4	2692.4	4.9	10	<0.9		<0.8	
5326.4	2702.4	14.5	5	<0.9		5.4	15
5264.8	2764.0	2.3	25	15.7	10	<0.8	
5232.6	2796.2	4.5	10	<0.9		1.4	60
5196.0	2832.8	<0.5		3.2	30	<0.8	
5173.6	2855.2	<0.5		<1.0		2.0	20
5166.5	2862.3	14.1	5	<0.9		5.0	20
5148.7	2880.1	1.3	40	11.7	10	<0.8	
5087.0	2941.8	4.4	10	<0.9		<0.8	
5077.8	2951.0	11.6	5	<0.9		11.7	10
5048.8	2980.0	6.1	10	4.0	20	2.9	25
5000.4	3028.4	8.5	10	<0.9		<0.8	
4985.8	3043.0	6.3	10	2.2	50	4.5	20
4965.1	3063.7	2.0	20	3.1	35	2.3	20
4952.3	3076.5	1.8	20	30.0	10	6.4	10
4846.3	3182.5	10.4	10	7.1	25	14.2	10
4829.5	3199.3	<0.5		<1.0		6.4	15
4799.2	3229.6	<0.5		<1.0		21.9	5

<sup>a</sup> The level energies have an accuracy of  $\pm 1$  keV up to 2500 keV, and  $\pm 2$  keV above 2500 keV. In addition, the  $\gamma$ -ray energy scale has a systematic uncertainty of  $\pm 0.5$  keV due to the uncertainty in the value of the neutron binding energy ( $8028.8 \pm 0.5$  keV) (Ref. 14).

<sup>b</sup> The intensities are given in arbitrary units; the normalization is consistent among the three resonances.

<sup>c</sup> Complex peak not resolved in the resonance spectra.

contains about ~330 transitions and 60 levels. Lines which are placed twice in the scheme are marked with an asterisk (\*). Lines which show some broadening in the present spectra but could not be completely resolved are marked with a "c." Dashed transition lines mean either that the transition is questionable or that its energy does not fit well. As a criterion for a good fit we assumed that the level energy difference and the corresponding transition energy should not differ by more than 1.5 times the combined error. Dotted lines represent  $E0$  transitions. Their energies were taken from  $(n, ce)$  studies. The thickness of the arrows corresponds roughly to the intensity of the transitions.

The requirements made on levels to be included in the decay scheme were: (i) evidence from primary feeding in thermal or resonance capture or in  $\beta$  decay; (ii) at least two combining decay lines. There are a few exceptions which are discussed below. For some levels good evidence was found from primary transitions but no unambiguous decay could be established. They are not included in the level scheme, but are discussed briefly at the end of this section.

The given excitation energies are average values; the error is in general about two units on the last digit shown.

Spin assignments and limits were derived from all available information. The general criteria used for spin determinations were:

(i) Primary transitions in the resonances were considered as  $E1$  transitions (determining positive parity of the final state) only if their intensities were at least  $\frac{3}{4}$  of the average intensity per transition.<sup>37</sup>

(ii) It was assumed that no  $M2$  or  $E3$  (or higher multipolarity) transitions should occur between levels if  $M1$  or  $E2$  transitions to other levels are possible.

(iii) No transitions which were complex, questionable, or could be placed several times in the level scheme were used for spin limitations. Multipolarities were considered only if they were unambiguously established.

(iv) In some cases the "statistical" feeding of a level following neutron capture was used as an argument in favor of one of two spin choices. The "statistical" feeding is the summed  $\gamma$  intensity going out of a level minus the intensity of a transition feeding this level directly from the compound state. An analysis of this kind for the levels with known spins (see Sec. IV A) results in most cases in a decreasing population with increasing spin and excitation energy, as expected from statistical considerations.<sup>38</sup> Application of these systematics for levels with unknown spin seems therefore

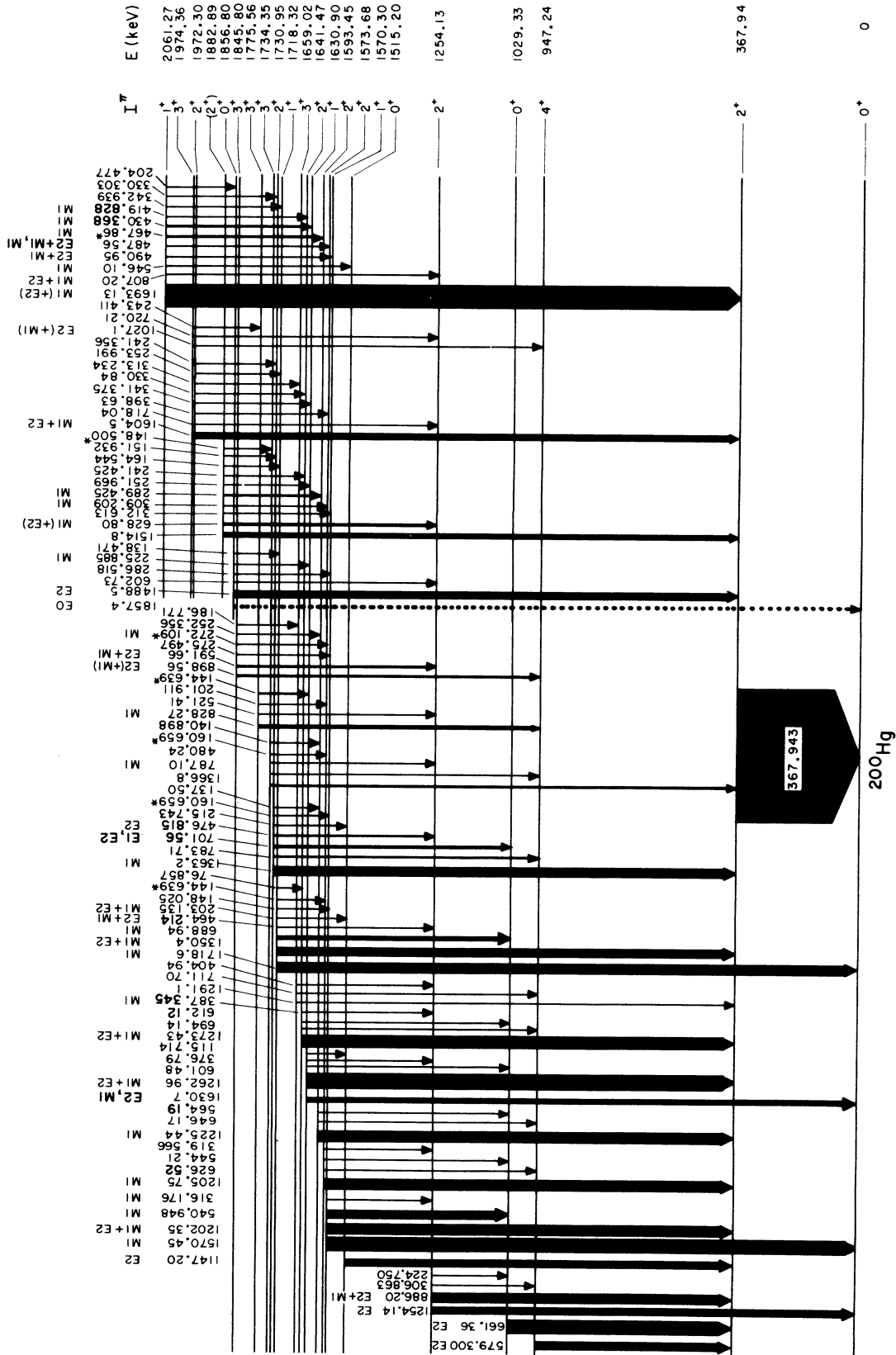


FIG. 4. Level scheme of  $^{200}\text{Hg}$ . Except for three (dotted)  $E0$  transitions, only those lines observed in the present measurements are included. A few others, not shown, are known from  $\beta$ -decay studies: They have been considered in making the spin assignments. Lines marked with \* are placed more than once in the level scheme. "c" indicates complex lines. Dashed lines are either questionable or fit badly in energy. The multipolarities shown are those given in Table I, i.e., no limitations implied by the level scheme itself are taken into account. The errors on the level energies are about 1-2 on the last digit shown.







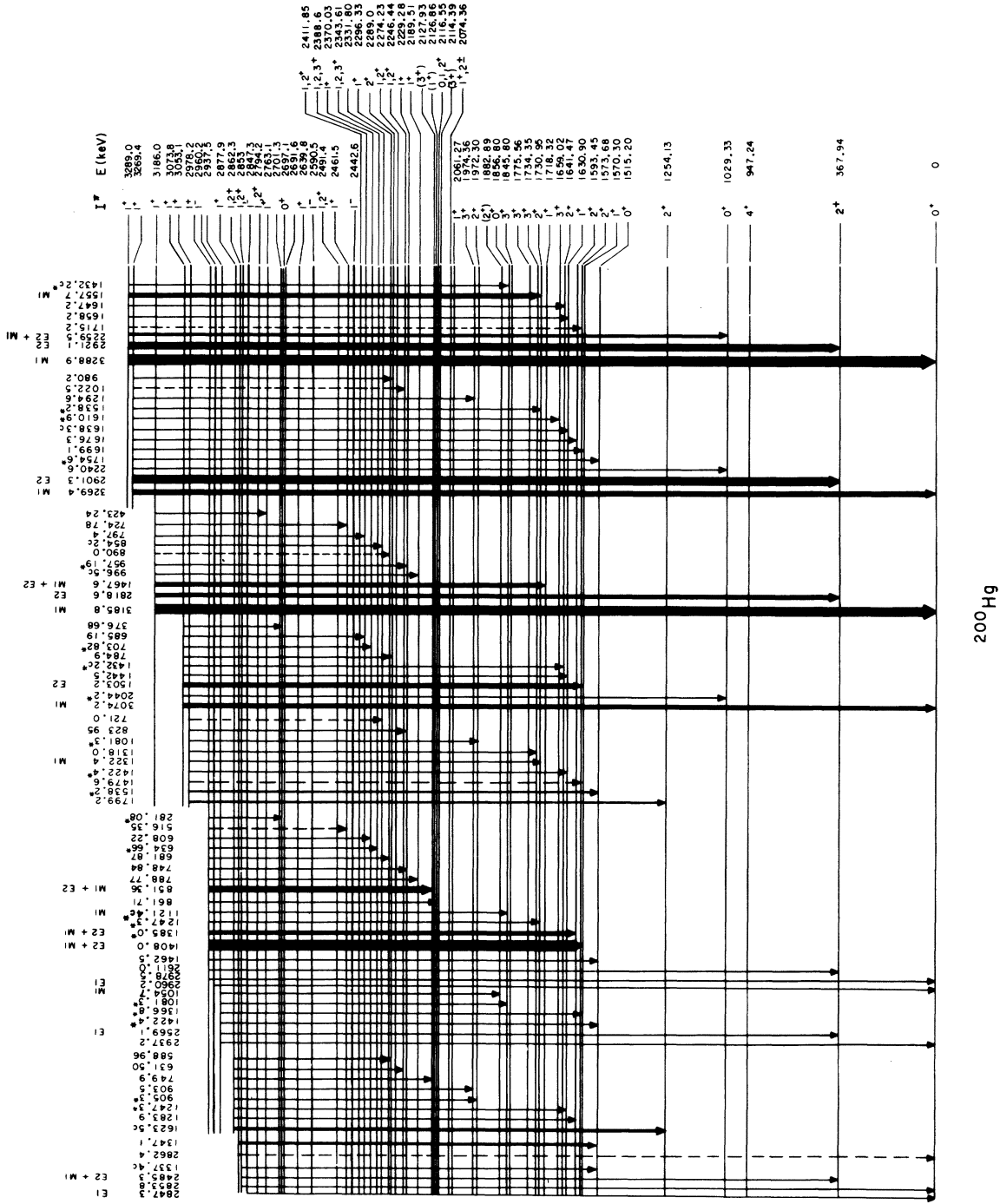


FIG. 7. Level scheme of <sup>200</sup>Hg. (See caption to Fig. 4.)

not unreasonable.

If several spins are shown for a level they are equally likely. Parentheses indicate some uncertainty in the spin assignment or refer to a less likely possibility. No spin-parity limits are given if there are more than three choices.

To check the correct placement of decay lines in the level scheme the  $\gamma$  branching ratios from thermal capture were compared with those obtained from  $\beta$ -decay studies and from our resonance measurement (see Sec. II F). These ratios for each level should be independent of its population in any of the three reactions.

In the following paragraphs some levels will be discussed which were either not known previously or for which considerable new information was gained from the present experiments. Below 2 MeV some well-known states are considered insofar as they are relevant to the later discussion.

*1029.3 keV (0<sup>+</sup>)*

The possibility of spin 2<sup>+</sup> for this level, first suggested by Sakai *et al.*<sup>2</sup> and Hopke, Naumann, and Spejewski,<sup>39</sup> was ruled out by recent measurements<sup>29</sup> in favor of spin 0<sup>+</sup> proposed by Maier *et al.*<sup>13</sup> and Schult *et al.*<sup>14</sup> The present measurement confirms the pure E2 character of the 661-keV line and is consistent with the nonexistence of a ground-state- $\gamma$  transition. The present  $\gamma$ - $\gamma$  angular-correlation measurement also yields unambiguously spin and parity 0<sup>+</sup> for this level. A possible E0 transition to the ground state was recently observed by Sakai, Kawakami, and Saito.<sup>40</sup>

*1254.1 keV (2<sup>+</sup>)*

Of the lines depopulating this level, the 306-keV and especially the 224-keV transition have been discussed many times as they seem not to fit any of the existing models. However, even with the considerably reduced errors in the present experiment their placement seems justified.

*1515.2 keV (0<sup>+</sup>)*

This level, though weakly populated in the  $\beta$  decay of <sup>200</sup>Tl, was first suggested by Komppa, Pakkanen, and Kantele.<sup>9</sup> They observed a 1147-keV line to be in coincidence only with the strong 368-keV line. A tentative spin assignment of (1, 2)<sup>+</sup> for the 1515-keV level was recently made in a <sup>200</sup>Au decay study.<sup>11</sup> In the thermal (*n,  $\gamma$* ) reaction the 1147-keV line is very strong and a strong coincidence was found. Several transitions from higher levels seen in our measurements confirm the state at 1515 keV. Our  $\gamma$ - $\gamma$  angular-correlation measurement shows a very pronounced anisotropy

for the cascade 1147-368 keV with  $R \sim 3$  (see Table II) which, together with the pure E2 character of the 1147-keV line,<sup>17, 18</sup> determines the spin 0<sup>+</sup> for this level with high certainty. In the (*n,  $\gamma$* ) spectrum a strong line of about 1515 keV is seen, which is, however, in coincidence with the 368-keV transition. Its placement in the level scheme (1882-368) is rather firmly established. This line shows an anomalously high conversion coefficient (Table I), which suggests that the electron line may contain a component corresponding to the 1515-keV E0 ground-state transition. The 1515-keV level is strongly populated in a (not explicitly evaluated) 264-eV 1<sup>-</sup> neutron resonance in <sup>199</sup>Hg.

*1570.3 keV (1<sup>+</sup>) and 1573.7 keV (2<sup>+</sup>)*

The 1202- and 1205-keV lines could be clearly separated in the present experiments, which allows the assignment of more precise multiplicities to these two lines (Table I) and establishes the deexcitation of the level doublet suggested by Schult *et al.*<sup>14</sup> A new line to the 4<sup>+</sup> state at 947 keV confirms the spin assignment of 2<sup>+</sup> for the higher level.

*1593.5 keV (2<sup>+</sup>)*

Previous  $\gamma$ - $\gamma$  angular-correlation measurements<sup>11</sup> as well as ours establish the spin 2<sup>+</sup> for this level, which is confirmed by our observation of a transition to the 4<sup>+</sup> state. It may be interesting to note the very similar (*n,  $\gamma$* ) decay and population of the 1573- and 1593-keV levels. In the  $\beta$  decay of <sup>200</sup>Au and <sup>200</sup>Tl the population of these two levels differs by more than one order of magnitude.<sup>5, 9</sup>

*1630.9 keV (1<sup>+</sup>), 1641.5 keV (2<sup>+</sup>), 1718.3 keV (1<sup>+</sup>),  
and 1730.9 keV (2<sup>+</sup>)*

These levels are well established by previous measurements and confirmed by the present one. Some additional weak transitions could be observed of which the 1630-1254 and the 1630-1515 may be of particular interest (see Discussion). For the stronger lines the multiplicities were revised in some cases. There was a disagreement between earlier (*n,  $\gamma$* ) and recent <sup>200</sup>Au decay studies<sup>11</sup> for the branching ratios of lines depopulating the 1630-keV level. The present measurement shows that two of these lines (1630, 601 keV) are members of now resolved doublets. Direct population of the levels at 1630 and 1718 keV from the 0<sup>-</sup> resonance at 129.7 eV confirms spin and parity 1<sup>+</sup> for them.

*1659.0 keV (3<sup>+</sup>), 1734.3 keV (3<sup>+</sup>)*

Both levels were suggested by Komppa, Pakkanen, and Kantele<sup>9</sup> with spin assignments (3, 4)<sup>+</sup>. In

addition to the proposed decay we observe new transitions to the 1254-keV level from the 1659-keV level and to the 1573- and 1593-keV levels from the 1734-keV level. Furthermore many feeding transitions were found, which gives further confidence in these levels. In both cases two feeding transitions from  $1^+$  levels eliminate  $4^+$ . A pure  $M1$  transition to the  $4^+$  state at 947 keV allows only  $3^+$  for the 1734-keV level. The same spin and parity is suggested for the 1659-keV level because of its low  $(n, \gamma)$  population (see Fig. 8).

1775.6 keV ( $3^+$ )

Several  $^{200}\text{Tl}$  decay studies have established a level at this energy.<sup>7,9,14</sup> In accordance with the spin  $3^+$ , recently confirmed by  $\gamma$ - $\gamma$  angular-correlation measurements,<sup>28</sup> the population in  $(n, \gamma)$  is relatively small. There is another line observed in the present experiment whose energy fits very well as the 1775- to 1630-keV transition. This rather strong 144-keV line should then be seen, however, in the  $\beta$  decay. Thus the placement of at least the main part of this line elsewhere in the level scheme (1718-1573) seems justified. Similar arguments indicate that almost the whole intensity of the 1408-keV line, which would fit in energy as the transition to the first excited state, is better placed as a deexcitation mode of the 2978-keV state.

1845.8 keV ( $3^+$ )

This level is well known from previous studies. The present experiment confirms the suggested decay and adds two new lines to the 1570- and the 1659-keV levels. The spin assignment  $3^+$  is supported by the observation of  $M1$  admixtures in the 898-keV transition to a  $4^+$  level and in the 591-keV line to a  $2^+$  level, although it should be noted that the multipolarity is not quite certain in the first case.

1856.8 keV ( $0^+$ )

Conversion electrons for transitions of 1857 keV ( $E0$ ) and 1489 keV ( $E2$ ) were observed by Mampe *et al.*,<sup>18</sup> who suggested this  $0^+$  level. The present data confirm the state and yield additional information on its decay. We observe the 225-keV  $M1$  line to the 1630-keV  $1^+$  state but not the 204-keV line to 1641 keV reported by Mampe *et al.* New lines were found to the 1254-, 1570-, and 1718-keV levels.

1882.9 keV ( $2^+$ )

The decay of this level has been revised and several new transitions have been found. The very

weak transition (not the same as our strong 935-keV line) to the  $4^+$  level seen only in the  $^{200}\text{Tl}$  decay<sup>9</sup> suggests  $I^\pi \geq 2^+$ . The  $(n, \gamma)$  population seems too high for a  $3^+$  level (see Fig. 8), which makes  $2^+$  most likely.

1972.3 keV ( $2^+$ ), 1974.4 keV ( $3^+$ )

Both levels were previously known<sup>9</sup> without spin assignments. A great number of new lines depopulating these levels were observed in the present study. The 1972-keV level is fed directly from the 33.5-eV  $1^-$  resonance, indicating  $I^\pi \leq 2$ . A  $0^+$  assignment for this level can be excluded, because of a line to a  $3^+$  state and the  $M1$  component in the 1604-keV transition. The  $\log ft$  values for  $1^+$  states populated from the  $^{200}\text{Tl}$   $\beta$  decay seem to be consistently high ( $>8.3$ ). Therefore, the relatively low  $\log ft$  value of 7.6 makes  $1^+$  less likely than  $2^+$  for the 1972-keV state. Another argument for a  $2^+$  assignment is the  $(n, \gamma)$  population which agrees very well with expectations (see Fig. 8). For the 1974-keV level spins 0 and 1 are excluded because of the transition to the  $4^+$  state [recently measured to be  $E2(+M1)$ ]<sup>38</sup>, and spin 4 is eliminated because of feeding transitions from two  $1^+$  levels. Of the remaining possibilities,  $3^+$  seems favored over  $2^+$  because of the very low  $(n, \gamma)$  population.

2074.4 keV ( $1^+, 2^+$ )

This previously unknown level is populated in the 175-eV  $1^-$  resonance. This fact in combination with the transition observed to a  $3^+$  state limits the spin possibilities.

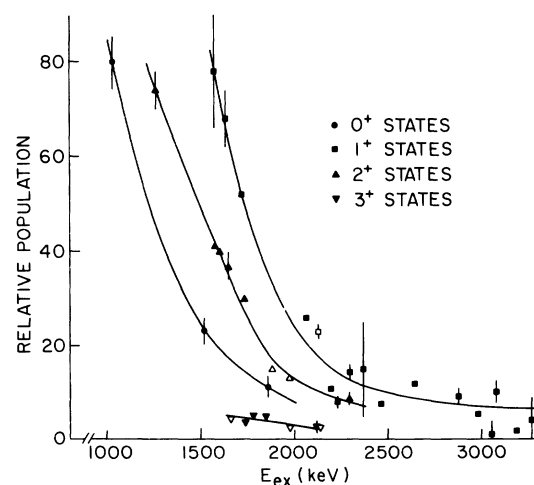


FIG. 8. Relative  $(n, \gamma)$  population of levels in  $^{200}\text{Hg}$ . Typical errors are given for some of the points. Open symbols indicate that the spin assignments for the associated levels were partly derived by using their population (see text).

2116.6 keV (0, 1, 2<sup>+</sup>)

A primary transition in the 175-eV 1<sup>-</sup> resonance leads to this new level. Its decay by strong low-energy transitions ( $M1$  and  $M1 + E2$ ), to the 1630- and 1718-keV 1<sup>+</sup> levels implies positive parity. It may be interesting that this level does not decay to the ground or first excited state as do most of the others.

2126.9 keV (1<sup>+</sup>), 2127.9 keV (3<sup>+</sup>)

The assumption of two closely spaced levels instead of the one previously suggested at 2127.2 keV<sup>9</sup> solves the discrepancies of the  $\gamma$  branching ratios in the ( $n, \gamma$ ) and  $\beta$  decay process. From this comparison it follows that most of the 1759-keV line must belong to the lower and most of the 872-keV line to the upper level. Both lines appear to be broad in the present ( $n, \gamma$ ) spectrum. As can be seen from the decay scheme many other closely spaced transitions, not previously resolved, support the two levels. Multipolarities for a number of these were determined. The decay of the two levels allows only  $I^\pi = 1, 2^+$  for the lower one and  $I^\pi = 2, 3^+$  for the upper one. As their ( $n, \gamma$ ) population differs by about one order of magnitude they cannot have the same spin. Assuming 1<sup>+</sup> for the 2126-keV level and 3<sup>+</sup> for the 2127-keV level, a very good agreement between the measured and expected population is achieved (Fig. 8).

2189.5 keV (1<sup>+</sup>)

A state near this energy was suggested in earlier neutron resonance studies.<sup>15, 16</sup> We also observe strong primary transitions in the two 1<sup>-</sup> resonances. 11 transitions are found to depopulate the level. The  $M1$  line to the ground state defines spin and parity 1<sup>+</sup>.

2229.3 keV (1<sup>+</sup>)

Primary transitions in thermal capture and in the 129-eV resonance define a level at about this energy. The ( $n, \gamma$ ) decay suggested by Mampe *et al.*,<sup>18</sup> however, is found to be in disagreement with the present results. Komppa, Pakkanen, and Kantele<sup>9</sup> observed the 975-keV line and transitions to the ground and first excited states. The latter two are below our detection limit. Spin and parity 1<sup>+</sup> for this level are suggested because of the strong primary transition in the 0<sup>-</sup> resonance.

2246.4 keV (1, 2<sup>+</sup>)

There is no evidence from the present data for a level at  $2248.8 \pm 0.3$  keV as suggested by Mampe *et al.*<sup>18</sup> The large error on the primary transition

energy observed by this group would be consistent with direct population of the present 2246 level. We observe direct transitions in the two 1<sup>-</sup> resonances. Positive parity and  $I \neq 0$  for this level is required by the  $M1 + E2$  transition to 1<sup>+</sup> at 1570 keV.

The level at 2259.1 keV suggested by Mampe *et al.*<sup>18</sup> based on a ground-state transition cannot be confirmed as the 2259-keV line is found to be in coincidence with the 368-keV transition.

2274.2 keV (1, 2<sup>+</sup>), 2289.0 keV (2<sup>+</sup>)

These two levels were found in the <sup>200</sup>Tl decay.<sup>9</sup> In both cases only transitions to the ground and first excited state were observed and no spin was given. In the present studies the ground-state transitions are below the detection limit but many lines to other states were found. For the 2274-keV level positive parity and spin limits can be derived from the  $E2$  transition to the 368-keV level, the direct feeding in a 1<sup>-</sup> resonance (which excludes 3<sup>+</sup>), and transitions to 3<sup>+</sup> levels (which excludes 0<sup>+</sup>). The 2289-keV level decays to the ground state (see above) and to the 4<sup>+</sup> state which allows only a 2<sup>+</sup> assignment.

2331.8 keV, 2343.6 keV (1, 2, 3<sup>+</sup>),  
2388.6 keV (1, 2, 3<sup>+</sup>)

These three levels were suggested by Komppa, Pakkanen, and Kantele.<sup>9</sup> However, only the transition to the first excited state was known in each case.

2411.9 keV (1, 2<sup>+</sup>)

In the present resonance spectra relatively strong primary transitions to this level in two 1<sup>-</sup> resonances are observed. The spin can be limited by the observation of decay lines to 0<sup>+</sup> and 3<sup>+</sup> levels. The level may be identical with one reported by Rae *et al.*<sup>15</sup> at 2418 keV.

2461.5 keV (1<sup>+</sup>), 2491.4 keV (1, 2<sup>+</sup>)

Mampe *et al.*<sup>18</sup> observe conversion lines from primary transitions to levels at 2460.5 and 2489.4 keV. Although the tentative decay cannot be confirmed, these could be the levels in question. Mampe's tentative spin assignment for the 2461-keV level is supported by a primary transition which we observe in the 0<sup>-</sup> resonance. The 2491-keV level is fed by the strongest transition from the 1<sup>-</sup> resonance at 175 eV. As we also observe a transition from this level to two 3<sup>+</sup> states, 1<sup>+</sup> or 2<sup>+</sup> are the only possible spin values.

2691.6 keV, 2701.3 keV

Two primary transitions in the present  $(n_{\text{res}}, \gamma)$  measurements lead to excitation energies of 2692 and 2701 keV. Both appear in the 33-eV  $1^-$  resonance. A number of combinations support these levels.

2697.1 keV ( $0^+$ )

Relatively few  $E0$  transitions were observed in the  $(n, ce)$  spectrum (see Sec. II F). Two of them, if built on the 1029- and 1515-keV  $0^+$  levels, respectively, define a new level at 2697 keV, which must also be  $0^+$ . The probability that this is accidental is very small.

2763.1 keV ( $1^+$ )

This level was observed by Alves *et al.*<sup>16</sup> Its decay, previously unknown, could now be established. Spin and parity  $1^+$  for the state are implied by the strong feeding in the  $0^-$  resonance.

2794.2 keV ( $1, 2^+$ )

This previously unknown level is fed in the 33-eV  $1^-$  resonance. Its decay to a  $1^+$  level (1630 keV) by a  $M1(+E2)$  transition suggests a  $0, 1, 2^+$  assignment. Although the observed ground-state transition and a transition to a  $3^+$  state are complex, the probability that both lines are placed incorrectly is very small. Under this assumption  $I=0$  seems rather unlikely.

2853 keV ( $1, 2^+$ )

This new level is fed, although relatively weakly, in the 175-eV  $1^-$  resonance. Spin and parity for it can be further limited by the observation of a ground-state transition and the  $E2 + M1$  multipolarity of the transition to the 368-keV level.

2862.3 keV ( $1, 2^+$ )

We suggest this level on the basis of rather strong primary transitions in both  $1^-$  resonances. The intensities suggest positive parity. Two transitions to  $0^+$  levels exclude spin 0. The existence of the ground-state transition, though questionable in thermal capture, is confirmed in the low-energy resonance capture spectrum.

2877.9 keV ( $1^+$ )

The 1147-keV line was previously thought to lead from this level to the 1730-keV state.<sup>14</sup> With this assumption, however, the intensity balance rule for the latter would be violated. Besides, the

placement of the 1147-keV line as the 1515-368 transition is rather definite.

2937.5 keV

This level is seen in the 33-eV resonance. However the decay transitions ascribed to it do not allow a parity assignment as we have placed both an  $E1$  and a  $M1$  line as possible deexcitations. Clearly one of the two must be incorrect.

2442.6 keV ( $1^-$ ), 2590.5 keV ( $1^-$ ),  
2847.3 keV ( $1^-$ ), 2960.2 keV ( $1^-$ )

Perhaps with the exception of the first,<sup>18</sup> these levels were previously unknown. Their common feature is that they are all based on relatively strong transitions which were found not to be in coincidence with the 368-keV line. As pointed out earlier, the decay of all levels below 3.3 MeV eventually feeds the 368-keV level. The possibility that the above lines are built onto levels above 3.3 MeV cannot be excluded but seems very unlikely, as these states have then to decay exclusively to the ground state. We therefore conclude that the four transitions are ground-state transitions. As their multipolarity was found to be  $E1$ , they define  $1^-$  initial states. There may be some other weaker lines depopulating these states, but their large energy errors lead to ambiguous choices and they are therefore not included in the level scheme. In the case of the 2960-keV level a strong 1706-keV line (possibly  $E1$ ) would fit as a transition to the 1254-keV level. However, this line is already placed elsewhere in the level scheme (2074-368). Although these levels do not meet the formal requirements given above, we consider them rather definite based on the present arguments.

Above ~3 MeV only such levels were included in the level scheme which were strongly fed by primary transitions in thermal-neutron capture. All of them were found earlier and assigned to be  $1^+$ . However, a great amount of new information on their decay was added by the present experiments. Of the 63 transitions now placed as to depopulating the highest six levels, only 16 were placed identically in earlier studies.<sup>14, 18</sup>

#### Other levels

Evidence for several other levels below 3 MeV was found, but no good decay (see criteria above) could be established for them. They are therefore not included in the level scheme. We have summarized them in Table IV, showing also the experimental evidence for each.

TABLE IV. Further levels in  $^{200}\text{Hg}$ .

Exc. energy (keV)	Spin	Evidence
2563		$1^-$ res.
2833	$1^+$	$0^-$ res.
2951	$0, 1, 2^+$	$2 \times 1^-$ res.
2954	$1^+, 2^+$	<i>g.s.</i> trans.

## IV. DISCUSSION

## A. Statistical population of levels

In the  $(n, \gamma)$  process low-lying levels are fed by  $\gamma$  decay of the compound state in a single-step process (primary transitions) or in a cascading process which involves two or more steps. In particular, in the latter case influences of nuclear structure on the transition rates may be largely obliterated and the feeding of a level may therefore be described in a statistical way. The population should then depend only on statistical properties of the nucleus (level density) and on general considerations about transition probabilities (Weisskopf estimate, systematics of hindrance factors). An outline of this concept is given by von Egidy,<sup>38</sup> who also did rather successful calculations for several nuclei. The general result of these calculations is that one can describe the spin dependence of the level population by a smooth curve which peaks at about the initial compound spin. One also expects a rapid decrease of the population with increasing excitation energy for levels of the same spin.

An empirical analysis of this kind was made for  $^{200}\text{Hg}$ . The population of a level was obtained by summing up the total intensity of depopulating lines. This method gives a lower limit which is reasonably close to the real value, if, as in the present case, most lower levels with similar spin values are known. Since we only want to consider the level feeding by cascades, the primary feeding was subtracted.

The results are shown in Fig. 8. For the spin values 0, 1, 2, and 3 the relative level population is plotted versus excitation energy. The filled symbols indicate levels for which the spin could be unambiguously derived from other than population arguments. Open symbols represent levels for which the decay properties allowed more than one spin possibility. The four curves are clearly displaced up to about 2.2 MeV and show the theoretically expected trend. Above this energy the curves overlap and the deviations from a smooth behavior are greater. The latter is partly due to the fact that high-lying levels may decay by additional lines which are below our detection limits.

These can contain a greater fraction of the decay intensity than similar lines from lower levels which usually decay via a few very dominant transitions. With increasing excitation energy one would also expect a gradual breakdown of the simple picture as the condition of several stage cascade feeding is not satisfied any more. This seems particularly obvious for the  $1^+$  states above 3 MeV which are almost exclusively fed by primary transitions. The spin dependence of the population is shown for three different excitation energies in Fig. 9(a). The peaks of the curves which occur at spin 1 become less pronounced the higher the level energy becomes, i.e., the fewer stages there are between the compound state and the level of interest. This is expected from a very simple qualitative consideration shown in Fig. 9(b). It demonstrates schematically the cascading process starting from a 0 compound spin which is the dominant compound spin for thermal-neutron capture in  $^{199}\text{Hg}$  and assuming dipole transitions of the same kind. For the sake of simplicity we also allowed  $0-0$   $E0$  transitions to occur with a strength equal to the dipole strength. The population is determined by simply counting the number of possible feeding branches. As can be seen the peak at spin 1 in the case of four cascading stages between compound and final state ( $\nu = 4$ ) disappears in the case of two stages ( $\nu = 2$ ).

The very systematic behavior of the population in  $^{200}\text{Hg}$  can be used as an additional tool for making spin assignments. For example spins for levels at 1659, 1882, 1972, 2126, and 2127 keV were determined partly using populating arguments (see Sec. III). It is also possible to estimate detection limits for states in terms of spin and excitation energy. From Fig. 8 one would not expect to see any spin-3 states above 2.5 MeV in the thermal  $(n, \gamma)$  reaction.

## B. Negative-parity states

In even-even nuclei just before closed shells, the noncollective low-lying excitations with low spins are expected and are found to be of positive parity.<sup>41</sup> The simplest mechanism to create negative-parity levels is an excitation across the shell gap. Since the low-spin shell-model orbits generally lie high in their respective shells, these low-spin negative-parity excitations would require at least the shell-gap energy and usually a major fraction of the energy width of the next shell. Another simple mechanism to form negative-parity states is via particle-hole excitations involving the so-called unique parity high-spin shell-model orbit. These excitations do not require crossing the shell gap but at the same time cannot couple

to very low spins within the spherical shell model.

In the Hg region, excitations of the former type may be expected near 6 MeV. The latter type may occur quite low in energy but with spins not lower than 4 for proton states or 2 for neutron levels. Several states with  $I \geq 5^-$  have previously been located in the decay of  $^{200}\text{Au}^m$ .<sup>42</sup> Due to the population systematics discussed above we would not expect to observe these states.

In view of these ideas it is interesting to find at least four  $1^-$  states in  $^{200}\text{Hg}$  between 2400 and 3000 keV. We have considered the various couplings that can lead to such states. The simplest that seem feasible are those of the form

$$[\pi(h_{9/2}d_{3/2}^{-1})^{I=3}\nu(f_{5/2}^2)^{I=2}(p_{1/2}^{-2})^{I=0}]^{I=1}.$$

This excitation takes advantage of the small pairing energy near closed shells to recouple spins and the attractive proton particle-hole residual interaction for excitations across the gap which has been found to be  $\sim -330$  keV from comparison of 2p-1h states in  $^{209}\text{Bi}$  and 1h states in  $^{207}\text{Tl}$ .<sup>43</sup>

The calculated energy for states of this form is  $\sim 4200$  keV.<sup>44</sup> The analogous neutron excitations are at slightly higher energies due to two nearly offsetting effects. The energy gap is somewhat smaller but, on the other hand, there is no energy gained from the neutron particle-hole interaction. The latter is known to be  $\sim 0$  from the closeness of the neutron pairing vibration in  $^{208}\text{Pb}$  to the energy predicted in the simple harmonic phonon approximation.<sup>45</sup>

Since these states are expected only above 4 MeV one is thus led to consider more complicated excitations and the following examples can be con-

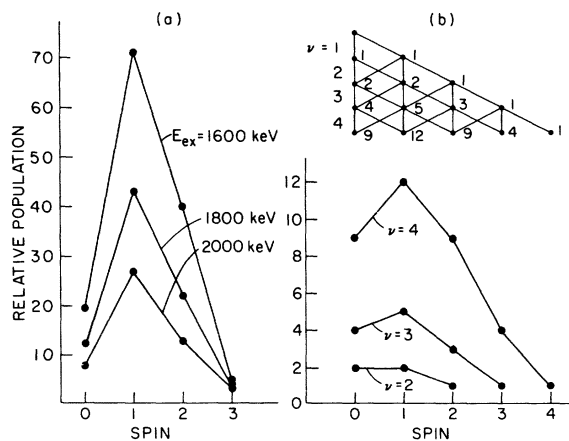


FIG. 9. (a) Spin dependence of the population (experimental). (b) Schematic illustration of the spin dependence.  $\nu$  indicates the number of cascading transitions between the compound and the final state.

structed:

$$\{[(f_{5/2}^2)^{I=5}(p_{1/2}^{-1})]^{I=11/2}(i_{13/2}^{-1})^{I=13/2}\}_{\nu}^{I=1},$$

$$\{[(f_{5/2}^2)^{I=5}(p_{3/2}^{-1})]^{I=11/2}(i_{13/2}^{-1})^{I=13/2}\}_{\nu}^{I=1},$$

and

$$\{[(f_{5/2}^2)^{I=4}(p_{3/2}^{-1})]^{I=11/2}(i_{13/2}^{-1})^{I=13/2}\}_{\nu}^{I=1}.$$

The first should lie lowest, at a calculated energy of  $\sim 2200$  keV, and the others would be expected below 3.5 MeV. This low energy arises from the small pairing energy combined with the absence of excitations across the gap. These states should exist in  $^{202}, ^{204}\text{Hg}$  but not in  $^{206}\text{Hg}$  where  $N=126$ . It would be interesting to pursue the search for them in these isotopes. Analogous excitations of higher seniority, including recoupling of proton pairs to nonzero spins, should also be found at not much higher energies.

The introduction of excitations of the unique parity states forces alternative considerations, however, since such excitations in this mass region have recently been interpreted in terms of oblate deformations.<sup>46, 47</sup> In a deformed field the degeneracy of the  $i_{13/2}$  orbit is broken. For prolate deformations the low- $K$  (angular-momentum projection on the nuclear symmetry axis) quantum number states drop in energy but for oblate deformations they rise.<sup>48</sup> Since the Fermi surface in  $^{200}\text{Hg}$  is above the  $i_{13/2}$  orbit, then for oblate deformations the low-spin excitations involving this orbital will occur at a relatively low excitation energy. The same argument applies to the proton  $h_{11/2}$  orbital. Two quasiparticle states with  $I^\pi = 1^-$  in  $^{200}\text{Hg}$  would then easily be formed by exciting the low  $K$   $\pi(h_{11/2})$  or  $\nu(i_{13/2})$  orbitals from the nearby  $\pi(s_{1/2}$  or  $d_{3/2})$  or  $\nu(p_{1/2}, p_{3/2}, f_{5/2})$  orbitals, respectively. This construction of  $1^-$  levels is an attractive hypothesis since one-particle  $E1$  transitions such as  $\frac{1}{2}^- [501] \rightarrow \frac{1}{2}^+ [660]$  or  $\frac{1}{2}^- [521] \rightarrow \frac{3}{2}^+ [651]$  (in Nilsson-model terminology) would have the typical  $n_z$  hindrance of  $E1$  transitions in deformed nuclei.<sup>49</sup>

Two related  $1^-$  excitations are the  $K=0$  and 1 oblate octupole vibrations. For oblate deformations in this mass region these octupole vibrations should in fact occur lowest in energy<sup>50</sup> (while for prolate deformations, the  $K=2, 3$  vibrations are lowest in the W and Os nuclei<sup>51</sup>). The  $I^\pi K=1^-$  (0 or 1) vibrations will be collective states dominated, probably, by linear combinations of excitations of the type mentioned in the previous paragraph involving for one quasiparticle a low- $K$  excitation of the  $\nu i_{13/2}$  or  $\pi h_{11/2}$  orbital. Again, one would expect these  $1^-$  levels to decay by  $E1$  transitions to the ground state.<sup>50</sup>

Another mode of  $1^-$  excitation is of interest. Re-



cently a sequence of  $5^-$ ,  $7^-$ ,  $9^-$ , and  $11^-$  levels with enhanced cascading  $E2$  transitions has been proposed<sup>42</sup> as a "collective band" in  $^{200}\text{Hg}$ . (Similar sequences of high-spin negative-parity levels have been found throughout the  $A=190-200$  region.<sup>53</sup>) The experimental evidence from the spin sequence, rotational energies, and  $\beta$ -decay feeding favors an interpretation<sup>42</sup> of the *intrinsic* structure of this band as involving (in the language of Refs. 53 and 54) a low-spin (e.g.,  $p_{3/2}$ ) quasiparticle excitation and a decoupled hole excitation of the  $i_{13/2}$  shell. This is qualitatively different from the simple oblate deformed two-quasiparticle  $1^-$  excitations discussed above. The *rotational* excitations of the band would be those of the even-even core somewhat modified by the presence of a partially decoupled two-quasiparticle state.<sup>42</sup> For the Fermi surface above the  $i_{13/2}$  level (as in  $^{200}\text{Hg}$ ) this interpretation requires<sup>54</sup> the oblate deformations deduced<sup>46, 47</sup> in the Hg region.

Experimentally the  $5^-$  "band-head" decays<sup>42</sup> by a transition to the 947-keV  $4^+$  level which is in itself well described as an excitation in the core-coupling scheme (see Sec. IV C). It is therefore reasonable to expect<sup>55</sup> a  $1^-$  level to arise from the coupling of these two intrinsic excitations. In the harmonic approximation its energy will be  $\approx 2800$  keV ( $E_{5^-} + E_{4^+}$ ). This is near the energy of several of the  $1^-$  levels observed in the present experiment.

#### C. Comparison with core-coupling calculations

Covello and Sartoris<sup>23</sup> have performed theoretical studies of the low-lying levels in  $^{200}\text{Hg}$ . They calculated states arising from coupling the two-proton holes in the  $3s_{1/2}$ ,  $2d_{3/2}$ ,  $1h_{11/2}$ , and  $2d_{5/2}$  shells to harmonic surface vibrations with up to three phonons and predict their excitation energies and decay properties. As their calculations do not include individual neutron states or other, more complicated, excitations, one should find experimentally a great number of additional levels. It is clear that the core-coupling model may neglect important interactions but it is worthwhile to attempt to locate those states most accurately described by the model. In fact, such analyses were made in most of the previous studies of  $^{200}\text{Hg}$ . The suggested candidates<sup>9</sup> were:  $2_1^+$  368 keV,  $4_1^+$  947 keV,  $0_2^+$  1029 keV,  $2_2^+$  1254 keV,  $2_3^+$  1573 keV or 1642 keV,  $1_1^+$  1630 keV, and  $3_1^+$  1659 keV or 1734 keV, where the notation  $J_i$  indicates the  $i$ th state of that spin.

The identification of a new  $0^+$  level at 1515 keV, the revision of some branching ratios and multipolarities by the present studies, and the discovery of some new transitions alter these conclusions to

some extent. Tables V and VI show a comparison of the experimental energies and transition rates with the predictions. For most energies and transition rates a reasonable agreement with the model is achieved assuming the earlier candidates and choosing 1573 keV as  $2_3^+$  and 1659 keV as  $3_1^+$ . However, some striking discrepancies remain:

(i) The energy of the 1029-keV level differs more than 400 keV from the predicted value for the  $0_2^+$  state whereas in all other cases the difference is less than 200 keV. (It should be pointed out that a model by Taruishi<sup>56</sup> predicts the positions of the  $4_1^+$ ,  $0_2^+$ , and  $2_2^+$  levels fairly well, but fails at higher energies.)

(ii) The transitions from the 1254-keV  $2_2^+$  state to the 947-keV  $4_1^+$  and 1029-keV  $0_2^+$  states are experimentally too strong by a factor 10 and 100, respectively. In particular the latter discrepancy is very serious as the weakest predicted transition [ $B(E2)$  value] is the strongest observed depopulating the 1254-keV level.

(iii) The transition 1630 keV  $\rightarrow$  1254 keV has only about  $\frac{1}{5}$  of the predicted  $1_1^+ \rightarrow 2_2^+$  strength.

The assumption of the 1515-keV  $0^+$  level as the predicted second  $0^+$  state would considerably improve the energy agreement (see Table V) and remove the above-described discrepancy for the  $2_2^+ \rightarrow 0_2^+$  transition because we observe no 1515- $\rightarrow$  1254-keV transition. However, an additional discrepancy arises for the 1630-keV  $1^+$  level as the transition 1630 keV  $\rightarrow$  1515 keV is much too strong to be the  $1_1^+ \rightarrow 0_2^+$  transition, which is actually predicted with zero strength. Experimentally this transition is by far the strongest [ $B(M1)$  value] depopulating the 1630-keV level. This would suggest another choice for the  $1^+$  state. The 1570-keV level has no observed decay to the 1515-keV level as expected and the transition to the first and second  $2^+$  state are in good agreement with the theory. Although the ground-state transition is

TABLE V. Excitation energies of core-coupled states in  $^{200}\text{Hg}$ .

State	$E_{C-S}$ (keV) <sup>a</sup>	$E_{exp}$ (keV) <sup>b</sup>	$\Delta = E_{exp} - E_{C-S}$
$2_1^+$	410	368	-42
$4_1^+$	1120	947	-173
$2_2^+$	1290	1254	-36
$0_2^+$	1470	1515 1029	+45 -441
$1_1^+$	1680	1570 1631	-110 -49
$2_3^+$	1760	1573	-187
$3_1^+$	1800	1659	-141

<sup>a</sup> The theoretical energies are taken from Covello and Sartoris, Ref. 23.

<sup>b</sup> Two sets of experimental candidates for the core-coupled states are given which differ by the choice of the  $0_2^+$  and  $1_1^+$  levels (see text).

much stronger than predicted, its experimental  $B(M1)$  value is at least of the same order as that of others depopulating the 1570-keV level. We therefore feel that the 1515- and the 1570-keV levels are the best choices for the predicted  $0_2^+$  and  $1_1^+$  states, respectively. In this case not only is the decay in reasonable agreement with the model, but also the energies of the states are close to the predicted values.

#### D. Bubble nuclei

In a recent series of studies<sup>24, 57-60</sup> the existence of a reduced central density (bubble) has been predicted for a number of nuclei, including  $^{200}\text{Hg}$ . In

this nucleus the bubble is calculated to occur in the ground-state configuration. The reduction of the central density to ~50% of its normal value emerges from a self-consistent Hartree-Fock calculation and relies essentially on the rise in energy of the  $\pi s_{1/2}$ ,  $\nu p_{1/2}$ , and  $\nu p_{3/2}$  shell-model orbits leading to a doubly magic bubble configuration with  $Z=80$  and  $N=120$ . Besides the one- and two-phonon vibrations of the outer surface, the model predicts<sup>61</sup> additional one- and two-phonon vibrations of the inner surface. The one-phonon excitation would be a  $2^+$  state at about 5 times the energy of the first  $2^+$  state. A  $\gamma$ -ray transition can change the phonon number by one and therefore, in the

TABLE VI. Comparison of predicted and experimental  $B(E2)$  and  $B(M1)$  values for low-lying states. For completeness the table includes results for states (1029 and 1630 keV) now thought (see text) *not* to correspond to calculated core-coupled states.

Transition <sup>a</sup>	Theor. values <sup>b</sup>			Cand. for initial level	$B(E2)$	Exp. values <sup>c</sup>		$ \delta_{\text{exp}} $
	$B(E2)$	$B(M1)$	$ \delta $			$B(M1)$		
$0_2^+ \rightarrow 2_1^+$	0.53			1515	†0.53			
$0_2^+ \rightarrow 2_2^+$	0.18			$0_2^+$	<0.95			
$1_1^+ \rightarrow 0_1^+$		0.01		1570		$1.48 \pm 0.25$		
$1_1^+ \rightarrow 2_1^+$		1.05	0.003	$1_1^+$		†1.05	$0.35^{+0.40}_{-0.25}$	
$1_1^+ \rightarrow 2_2^+$		1.00	0.004			$2.1^{+0.4}_{-0.8}$	$0 + 0.25$	
$1_1^+ \rightarrow 0_2^+$ (1515)		0				††		
$1_1^+ \rightarrow 0_2^+$ (1029)		0				$3.9 \pm 1.5$		
$2_2^+ \rightarrow 0_1^+$	0.12			1254	†0.12			
$2_2^+ \rightarrow 2_1^+$	0.97	0.31	1.7	$2_2^+$	$1.20 \pm 0.24$			$4^{+8}_{-1.4}$
$2_2^+ \rightarrow 4_1^+$	0.06				$0.7 \pm 0.2$			
$2_2^+ \rightarrow 0_2^+$ (1029)	0.036				$5.2 \pm 1.2$			
$2_3^+ \rightarrow 2_1^+$	0.16	1.07	0.15	1573	<0.07	†1.07		$0 + 0.12$
$2_3^+ \rightarrow 0_1^+$	0.007			$2_3^+$	<0.004			
$2_3^+ \rightarrow 4_1^+$	0.05				†0.05			
$2_3^+ \rightarrow 2_2^+$	0.20	0.25			$0.9 \pm 0.4$	$0.11 \pm 0.03$		
$2_3^+ \rightarrow 0_2^+$ (1029)	0.08				$0.08 \pm 0.02$			
$2_3^+ \rightarrow 0_2^+$ (1515)	0.08				††			
$3_1^+ \rightarrow 2_1^+$	0.18	0.15		1659	†0.18	†0.15		
$3_1^+ \rightarrow 4_1^+$	0.53	0.41		$3_1^+$	$0.90 \pm 0.30$	$0.23 \pm 0.08$		
$3_1^+ \rightarrow 2_2^+$	2.04	0.29			$1.1 \pm 0.5$	$0.09 \pm 0.04$		
$3_1^+ \rightarrow 2_3^+$	0.09	0.38			††	††		
$3_1^+ \rightarrow 1_1^+$ (1570)	0				††			
$3_1^+ \rightarrow 1_1^+$ (1630)	0				††			
$1_1^+ \rightarrow 0_1^+$		0.01		1630		$0.050 \pm 0.025$		
$1_1^+ \rightarrow 2_1^+$		1.05	0.003			†1.05	$0.25^{+0.30}_{-0.22}$	
$1_1^+ \rightarrow 2_2^+$		1.00		$1_1^+$		$0.18 \pm 0.05$		
$1_1^+ \rightarrow 0_2^+$ (1029)		0				$0.05 \pm 0.02$		
$1_1^+ \rightarrow 0_2^+$ (1515)		0				$36 \pm 15$		

<sup>a</sup> The notation  $0_1^+$ ,  $0_2^+$ , etc., corresponds to the notation given in Ref. 23. In some cases two different final states (in parentheses) are considered.

<sup>b</sup> Theoretical values are from Ref. 23.

<sup>c</sup> The  $B(E2)$  and  $B(M1)$  values are relative and normalized to the theoretical values using transitions marked with †. †† means that only very crude limits can be found for these transitions, which are, however, in agreement with the predictions. Experimental values are derived in some cases assuming alternatively pure  $E2$  and  $M1$  character for transitions whose multipolarity is not known.

simplest model, the two one-phonon  $2^+$  states will decay solely to the ground state. The two-phonon levels will decay only to their respective  $2^+$  one-phonon excitations. It is likely, however, that extensive mixing will significantly modify these simple rules.

The following points can nevertheless be made. The lowest possible  $2^+$  level (excluding 368 keV) in  $^{200}\text{Hg}$  observed in the present study to decay to the ground state is at 2794 keV. This energy would be significantly greater than the  $5 \times 368$  keV expected for a vibration of the inner bubble surface.

However, one might argue that the  $^{200}\text{Hg}$  ground state is unlikely to be a doubly magic bubble configuration because of the low energy of the first  $2^+$  level at 368 keV. (In fact this is the lowest excited-state energy in any even-even Hg isotope.) Therefore one can speculate whether or not a bubble configuration exists in some other low-lying  $0^+$  state in  $^{200}\text{Hg}$ . The discovery of the 1515-keV  $0^+$  state and its assignment (see Table VI) as the  $0_2^+$  core-coupled level leaves a  $0^+$  level at 1029 keV whose structure is unknown. If only one low-lying  $0^+$  state is present in  $^{198, 202}\text{Hg}$  then the 1029-keV "extra"  $0^+$  level in  $^{200}\text{Hg}$  would be a possible candidate for a bubble configuration. The 1593-keV state would be the lowest available  $2^+$  state not accounted for by the core-coupling model. The  $1593 - 1029 = 564$  keV energy difference would place the predicted inner surface vibrational  $2^+$  energy at  $\sim 3750$  keV, or outside the range of the present data. It is fruitless to extend these speculations, however, pending a study of  $^{202}\text{Hg}$  which is now in progress.<sup>62</sup> A final point to note, of presently unknown significance, is that the 1570-keV  $1^+$  state decays most strongly by a transition to the 1029-keV level.

## V. CONCLUSIONS

The  $(n, \gamma)$  reaction on  $^{199}\text{Hg}$  has been studied with a variety of techniques and a relatively complete level scheme for low-spin states below 3.3 MeV has been constructed. Many new transitions were placed and spin-parity assignments made. Several new levels, including a  $0^+$  state at 1515 keV were discovered.

The following principal conclusions were drawn from the data and level scheme:

(i) The intensity of secondary feeding was found to depend smoothly on excitation energy and spin and provided a useful aid in making spin assignments.

(ii) Due primarily to the discovery of the new  $0^+$  level at 1515 keV and the reassignment of a different  $1^+$  level as a model state, the core-coupling calculations of Covello and Sartoris were found to

provide a better description of the levels below 1.8 MeV than had previously been thought.

(iii) However, a  $0^+$  level at 1029 keV then remains unexplained. This may be of interest in connection with recent bubble nucleus calculations which predict  $^{200}\text{Hg}$  to have a low-lying bubble configuration. In regard to this model lower limits on the energies of possible vibrational levels were also obtained.

(iv) Four low-lying new  $1^-$  levels were detected between 2.4 and 3.0 MeV. It was possible to account for their low energies only by recourse to excitations of the unique parity orbits in terms of four-quasiparticle spherical excitations or of deformed two-quasiparticle and collective excitations. It is important to note that these latter structurally simple, low seniority interpretations involve the assumption of oblate deformations, at least for some states in  $^{200}\text{Hg}$ . This finding is consistent with and complements the conclusions of Refs. 46 and 47 for  $^{199}\text{Tl}$ .

These results suggest several future experiments. Experiments designed to search for  $1^-$  and  $0^+$  levels in neighboring isotopes would be useful. In particular, the conjecture of a bubble configuration for the 1029-keV level would seem to suggest the absence of a similar low-lying  $0^+$  excitation in  $^{198, 202}\text{Hg}$ . A study of the latter is in progress.

The position of  $^{200}\text{Hg}$  between the spherical nuclei near  $^{208}\text{Pb}$  and the suggested oblate configurations in  $^{199}\text{Tl}$  and the Pt isotopes suggests that it may be transitional in character. Single neutron transfer reactions leading to the  $1^-$  levels and the states below 1.8 MeV would be useful in probing the single-particle aspects of these levels. In particular they might reveal whether or not the negative-parity excitations ( $1^-, \dots, 5^-, 7^-$ ) are coexisting oblate configurations or whether such deformations characterize the nucleus as a whole. The success [see (ii) above] of the core-coupling model may suggest that at least the low-lying levels can be interpreted in terms of a spherical basis. The cross sections in  $(t, p)$  or  $(p, t)$  reactions could clarify the amplitudes of core-coupling configurations in these lower-lying levels.

## ACKNOWLEDGMENTS

We are grateful to a number of people for stimulating discussions. In particular these include Dr. P. J. Daly, Dr. F. S. Stephens, Dr. J. P. Vary, Dr. P. Vogel, Dr. C. Y. Wong, and Dr. G. Struble. We are especially grateful to Dr. W. R. Kane for help and advice in many phases of this work. We

thank Dr. H. Kraner for the loan of an intrinsic Ge detector used in the resonance capture measurements. One of us (D.B.) acknowledges partial support from the Technical University of Munich, and is grateful to Professor O. Schult, Dr. R. Koch,

and Dr. H. Baader of the Risø bent-crystal spectrometer group for their help and participation in those phases of these measurements. The assistance of M. Burger in the analysis of that data is also acknowledged.

- \*Work supported by U. S. Atomic Energy Commission.  
 †Permanent address: Physik Department E17, Technische Universität München, Munich, Germany.
- <sup>1</sup>C. J. Herrlander and T. R. Gerholm, *Nucl. Phys.* **3**, 161 (1957).
  - <sup>2</sup>M. Sakai, H. Ikegami, T. Yamazaki, and K. Saito, *Nucl. Phys.* **65**, 177 (1965).
  - <sup>3</sup>J. C. Roy and L. P. Roy, *Can. J. Phys.* **37**, 385 (1959).
  - <sup>4</sup>R. K. Girgis, R. A. Ricci, and R. Van Lieshout, *Nucl. Phys.* **14**, 589 (1960).
  - <sup>5</sup>O. W. B. Schult, W. R. Kane, and E. der Mateosian, *Phys. Rev.* **170**, 1055 (1968).
  - <sup>6</sup>M. Sakai, *J. Phys. Soc. Jap.* **26**, 879 (1969).
  - <sup>7</sup>R. Béraud, I. Berkes, J. Danfère, R. Haroutunian, M. Levy, G. Marest, and R. Rougny, *Phys. Rev.* **188**, 1958 (1969).
  - <sup>8</sup>M. Sakai, H. Kawakami, and K. Saito, *J. Phys. Soc. Jap.* **28**, 542 (1970).
  - <sup>9</sup>T. Komppa, A. Pakkanen, and J. Kantele, *Nucl. Phys.* **A163**, 513 (1971).
  - <sup>10</sup>H. Ton, G. H. Dulfer, J. Brasz, R. Kroondijk, and J. Blok, *Nucl. Phys.* **A153**, 129 (1970).
  - <sup>11</sup>H. Helppi and A. Pakkanen, *Z. Phys.* **255**, 385 (1972).
  - <sup>12</sup>L. V. Groshev, A. M. Demidov, V. Z. Ivanov, N. V. Lutsenko, and V. I. Pelekhov, *Izv. Akad. Nauk SSSR, Ser. Fiz.* **27**, 1377 (1963) [transl.: *Bull. Acad. Sci. Phys. Ser.* **27**, 1353 (1963)].
  - <sup>13</sup>B. P. Maier, U. Gruber, H. R. Koch, and O. W. B. Schult, *Z. Phys.* **185**, 478 (1965).
  - <sup>14</sup>O. W. B. Schult, W. R. Kane, M. J. Mariscotti, and J. M. Simić, *Phys. Rev.* **164**, 1548 (1967).
  - <sup>15</sup>E. R. Rae, W. R. Moyer, R. R. Fullwood, and J. L. Andrews, *Phys. Rev.* **155**, 1301 (1967).
  - <sup>16</sup>R. N. Alves, J. M. Kuchly, J. Julien, C. Samour, and J. Morgenstern, *Nucl. Phys.* **A135**, 241 (1969).
  - <sup>17</sup>O. W. B. Schult, W. Kaiser, W. Mampe, and T. von Egidy, *Z. Phys.* **218**, 95 (1969).
  - <sup>18</sup>W. Mampe, T. von Egidy, W. Kaiser, and K. Schreckenbach, *Z. Naturforsch.* **26A**, 405 (1971).
  - <sup>19</sup>M. J. Martin, *Nucl. Data B6*(No. 4), 387 (1971).
  - <sup>20</sup>R. F. Casten, E. Cosman, E. R. Flynn, O. Hansen, P. W. Keaton, Jr., N. Stein, and R. Stock, *Nucl. Phys.* **A202**, 161 (1973).
  - <sup>21</sup>R. A. Moyer, *Phys. Rev. C* **5**, 1678 (1972).
  - <sup>22</sup>G. Alaga and G. Jalongo, *Phys. Lett.* **22**, 619 (1966).
  - <sup>23</sup>A. Covello and G. Sartoris, *Nucl. Phys.* **A104**, 189 (1967).
  - <sup>24</sup>C. Y. Wong, *Phys. Lett.* **41B**, 451 (1972).
  - <sup>25</sup>H. R. Koch, M. A. Baader, D. Breitig, K. Mühlbauer, U. Gruber, B. P. Maier, and O. W. B. Schult, in *Neutron Capture Gamma-Ray Spectroscopy* (International Atomic Energy Agency, Vienna, 1969), p. 65.
  - <sup>26</sup>K. Mühlbauer, Dissertation, Technische Hochschule München, 1968 (unpublished).
  - <sup>27</sup>P. Bergvall, *Ark. Fys.* **16**, 57 (1960).
  - <sup>28</sup>J. Hattula, H. Helppi, and J. Kantele, *Z. Phys.* **241**, 117 (1971).
  - <sup>29</sup>K. E. G. Löbner, D. Rabenstein, and O. W. B. Schult, *Z. Phys.* **226**, 13 (1969); G. A. Bartholemew, S. I. H. Naqui, M. R. Gunye, and E. D. Earle, *Can. J. Phys.* **45**, 1517, 2063 (1967).
  - <sup>30</sup>H. Frauenfelder and R. M. Steffen, in *Alpha-, Beta-, and Gamma-Ray Spectroscopy*, edited by K. Siegbahn (North-Holland, Amsterdam, 1965).
  - <sup>31</sup>W. G. Winn and D. G. Sarantites, *Nucl. Instrum. Methods* **66**, 61 (1968).
  - <sup>32</sup>L. A. Sliv and J. M. Band, in *Alpha-, Beta-, and Gamma-Ray Spectroscopy* (see Ref. 30).
  - <sup>33</sup>R. E. Chrien and M. Reich, *Nucl. Instrum. Methods* **53**, 93 (1967).
  - <sup>34</sup>M. R. Bhat, B. R. Borrill, R. E. Chrien, S. Rankowitz, B. Soucek, and O. A. Wasson, *Nucl. Instrum. Methods* **53**, 108 (1967).
  - <sup>35</sup>*Neutron Cross Sections*, compiled by M. D. Goldberg, S. F. Mughabghab, S. N. Purohit, B. A. Magurno, and V. M. May, BNL Report No. BNL-325, 1966 (unpublished), 2nd ed., 2nd Suppl., Vol. IIA.
  - <sup>36</sup>L. M. Bollinger, R. E. Coffe, R. T. Carpenter, and J. P. Marion, *Phys. Rev.* **132**, 1640 (1963).
  - <sup>37</sup>L. M. Bollinger and G. E. Thomas, *Phys. Rev. Lett.* **18**, 1143 (1967).
  - <sup>38</sup>T. von Egidy, in *Neutron Capture Gamma-Ray Spectroscopy* (see Ref. 25), p. 541.
  - <sup>39</sup>P. K. Hopke, R. A. Naumann, and E. M. Spejewski, *Phys. Rev.* **177**, 1802 (1969).
  - <sup>40</sup>M. Sakai, H. Kawakami, and K. Saito, *J. Phys. Soc. Jap.* **28**, 542 (1970).
  - <sup>41</sup>E. U. Barranger, *Bull. Am. Phys. Soc.* **18**, 90 (1973).
  - <sup>42</sup>J. C. Cunnane, R. Hochel, S. W. Yates, and P. J. Daly, *Nucl. Phys.* **A196**, 593 (1972).
  - <sup>43</sup>P. D. Barnes, E. Romberg, C. Ellegaard, R. F. Casten, O. Hansen, T. J. Mulligan, R. Broglia, and R. Liotta, *Nucl. Phys.* **A195**, 146 (1972).
  - <sup>44</sup>We are grateful to J. P. Vary for some calculated particle-hole interaction energies within the major shells.
  - <sup>45</sup>R. A. Broglia, O. Hansen, and K. Riedel, to be published.
  - <sup>46</sup>J. O. Newton, S. D. Cyrilov, F. S. Stevens, and R. M. Diamond, *Nucl. Phys.* **A148**, 593 (1970).
  - <sup>47</sup>K. Nakai, *Phys. Lett.* **34B**, 269 (1971).
  - <sup>48</sup>S. G. Nilsson, *K. Dan. Vidensk. Selsk. Mat.-Fys. Medd.* **29**, No. 16 (1955).
  - <sup>49</sup>K. E. G. Löbner and S. G. Malmskog, *Nucl. Phys.* **80**, 505 (1966).
  - <sup>50</sup>P. Vogel, private communication.
  - <sup>51</sup>K. Neergaard and P. Vogel, *Nucl. Phys.* **A145**, 33 (1970).
  - <sup>52</sup>K. Krien, E. H. Spejewski, R. A. Nauman, and H. Hinkel, *Phys. Rev. C* **5**, 1751 (1972).
  - <sup>53</sup>F. S. Stephens, R. M. Diamond, J. R. Leigh, T. Kamimuri, and K. Nakai, *Phys. Rev. Lett.* **29**, 438 (1972).
  - <sup>54</sup>F. S. Stephens, R. M. Diamond, and S. G. Nilsson, *Phys. Lett.* **44B**, 429 (1973).

<sup>55</sup>F. S. Stephens, private communication.

<sup>56</sup>K. Taruishi, *Prog. Theoret. Phys.* 39, 53 (1968).

<sup>57</sup>K. T. R. Davies, C. Y. Wong, and S. J. Krieger, *Phys. Lett.* 41B, 455 (1972).

<sup>58</sup>C. Y. Wong, *Ann. Phys. (N. Y.)* 77, 279 (1973).

<sup>59</sup>K. T. R. Davies, S. J. Krieger, and C. Y. Wong, ORNL Report, 1973 (to be published).

<sup>60</sup>S. J. Krieger, K. T. R. Davies, and C. Y. Wong, in *Proceedings of the International Conference on Nuclear Structure*, edited by J. de Boer and H. J. Mang (North-Holland, Amsterdam, 1973), p. 56.

<sup>61</sup>C. Y. Wong, private communication.

<sup>62</sup>D. Breitig, R. F. Casten, G. W. Cole, W. R. Kane, and J. Cizewski, to be published.